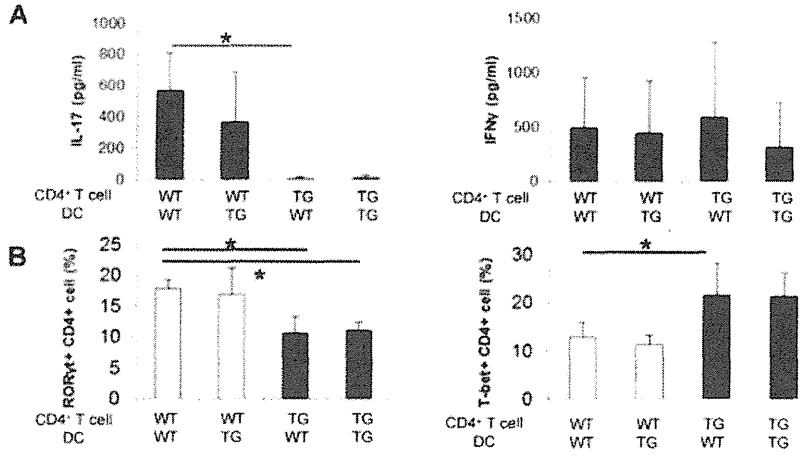

Figure 5. Impaired antigen-specific Th17 cell responses in T-bet–transgenic (Tg) mice with collagen-induced arthritis (CIA). Ten days after the first type II collagen (CII) immunization, CD4+ cells were isolated from draining lymph nodes of C57BL/6 (wild-type [WT]) mice and T-bet–Tg (TG) mice by positive selection using magnetic-activated cell sorting (MACS) with anti-CD4 monoclonal antibody (mAb). After treatment with mitomycin C, CD11c+ cells were isolated from the spleen by positive selection using a MACS system with anti-CD11c mAb. Criss-cross coculture for 72 hours was performed with 1×10^5 CD4+ cells and 2×10^4 CD11c+ cells in 100 μg/ml of denatured CII–containing medium. **A,** Levels of interleukin-17 (IL-17) and interferon-γ (IFNγ) in culture supernatants were measured by enzyme-linked immunosorbent assay. **B,** Expression of retinoic acid receptor–related orphan nuclear receptor γt (RORγt) and T-bet expression on CD4+ T cells were analyzed by intracellular staining. Representative data from flow cytometric analysis of the percentage of RORγt+ or T-bet+ cells in the CD4+ T cell subset are shown. Values are the mean ± SD of 3 mice per group. * = $P < 0.05$ by Student's *t*-test. DC = dendritic cells.

T-bet–Tg/IFNγ$^{-/-}$ mice (Figure 6). These results strongly support the view that inhibition of Th17 cell differentiation in T-bet–Tg mice cannot be due to overproduction of IFNγ, indicating that overexpression of T-bet directly suppresses Th17 cell differentiation in T-bet–Tg mice.

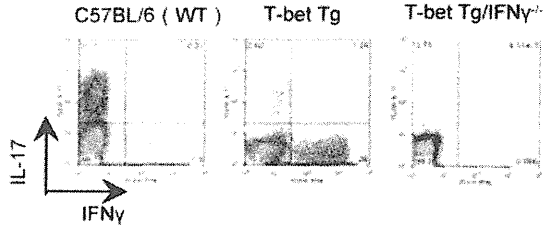

Figure 6. Suppressed expression of interleukin-17 (IL-17) by T-bet overexpression independently of interferon-γ (IFNγ) in T-bet–transgenic (Tg) mice. CD4+ T cells were isolated from the spleen of C57BL/6 (wild-type [WT]), T-bet–Tg, and T-bet–Tg/IFNγ$^{-/-}$ mice by magnetic-activated cell sorting and then cultured for 96 hours with soluble anti-CD3 monoclonal antibody (mAb), soluble anti-CD28 mAb, IL-6, and transforming growth factor β. IFNγ and IL-17 production by CD4+ cells was analyzed by intracellular cytokine staining. Numbers in each compartment are the percentage of cells secreting cytokines.

DISCUSSION

Recent studies showed that IL-17 plays a crucial role in the development of CIA (3) and other types of experimental arthritis (2). In contrast, it has been reported that IFNγ can suppress IL-17 production in vitro (16) and has antiinflammatory effects on the development of experimental arthritis (4,5). T-bet is a transcription factor known to induce the differentiation of naive CD4+ T cells to Th1 cells (8). Although the absence of T-bet can result in severe IL-17–mediated experimental autoimmune myocarditis via dysregulation of IFNγ (17), several studies have shown that T-bet is essential for the development of several models of autoimmunity, such as experimental autoimmune encephalitis (18,19), colitis (20), and diabetes mellitus (21). Nevertheless, the effect of T-bet expression on Th17 cell differentiation and function during arthritis remains unclear.

T-bet–Tg mice overexpress T-bet and mainly produce IFNγ in their T cells (14). Previous studies in T-bet–Tg mice suggested that overexpression of T-bet and a predominant Th1 response affect the pathogenesis of various diseases (14,22,23). To examine whether T-bet overexpression on T cells affects the regulation of

autoimmune arthritis, we induced CIA in T-bet–Tg mice and found marked suppression of CIA in T-bet–Tg mice.

To determine the reason for the low incidence of CIA in T-bet–Tg mice, we measured CII-reactive cytokine production and expression in vitro. IL-17 production from CII-reactive CD4+ T cells and *Il17a* expression were reduced in T-bet–Tg mice as compared with B6 mice. Although a predominant Th1 cell response was reported by Ishizuka et al (14), CII-specific IFNγ production was reduced in T-bet–Tg mice, and no significant difference was observed in *Ifng* expression between B6 mice and T-bet–Tg mice. Furthermore, *Il12a* expression was significantly higher in T-bet–Tg mice than in B6 mice, suggesting that overexpression of T-bet on T cells seems to affect innate immune cells, because the main producers of IL-12 are DCs and macrophages, not CD4+ T cells.

In criss-cross coculture experiments with CD4+ T cells and splenic DCs from B6 mice and T-bet–Tg mice, CII-reactive IL-17 production was also reduced even when CD4+ T cells from T-bet–Tg mice were cocultured with DCs from B6 mice, although there was no significant difference in IL-17 production by CD4+ T cells from B6 mice cocultured with DCs from either B6 mice or T-bet–Tg mice. In contrast, no difference in IFNγ production was observed under all coculture conditions examined. Moreover, suppression of RORγt expression and high expression of T-bet on CD4+ T cells were observed even when CD4+ T cells from T-bet–Tg mice were cocultured with DCs from B6 mice. These findings indicate that T-bet overexpression on CD4+ T cells might suppress CII-reactive IL-17 production resulting from suppression of RORγt expression in an IFNγ-independent manner, and that overexpression of T-bet has no direct effect on DC function.

CII-specific IgG levels correlate well with the development of arthritis (15). We observed significant suppression of CII-specific IgG production in the T-bet–Tg mice as compared with the B6 mice. A previous study showed that IL-17 is required for anti-CII antibody production (3). Therefore, the suppression of anti-CII antibody formation might be due to lower CII-reactive IL-17 production in T-bet–Tg mice.

To evaluate the low cytokine response to CII in T-bet–Tg mice, we analyzed lymphocytes obtained after immunization from draining lymph nodes and spleen. The percentage and absolute number of T cells tended to be lower in both the draining lymph nodes and spleen of T-bet–Tg mice compared with B6 mice. Moreover, significantly lower numbers of total thymocytes and an abnormal proportion of T precursor cells were observed in T-bet–Tg mice. The latter phenomenon could be due to T-bet transgene expression on double-negative thymic cells in T-bet–Tg mice. Because previous observations showed that T-bet interferes with GATA-3 function (11) and that GATA-3 was required for the development of early thymic T cells (24), one of the reasons for abnormal T cell development in the thymus might be the dysfunction of GATA-3 by overexpression of T-bet. These results suggest that overexpression of T-bet in thymic T cells affects T cell development, is responsible for the low number of T cells in spleen and lymph nodes, and is related to the low cytokine production against CII in T-bet–Tg mice.

To assess the effect of T-bet on CD4+ T cell differentiation in T-bet–Tg mice, we performed in vitro induction of Th17 cells. Analysis of T-bet–Tg mice showed a reduction in IL-17–producing CD4+ T cells and an increase in IFNγ-producing CD4+ T cells in spite of the condition favoring Th17 differentiation, which indicates suppression of Th17 cell differentiation and predominance of Th1 cell differentiation in vitro in T-bet–Tg mice. These results did not contradict the previous findings that the phenotype of polarized Th1 cells was not affected by Th cell–polarizing conditions (25). It is possible that suppression of CII-reactive IL-17 production in T-bet–Tg mice was not associated with IFNγ. For this reason, we generated T-bet–Tg/IFNγ$^{-/-}$ mice and performed in vitro induction of Th17 cells in these mice. Surprisingly, in T-bet–Tg/IFNγ$^{-/-}$ mice, the levels of IL-17–producing CD4+ T cells were also markedly reduced under Th17 cell differentiation–favoring conditions, indicating an IFNγ-independent suppressive pathway against Th17 cell differentiation. Although previous studies showed that suppression of Th17 cell differentiation was mediated through IFNγ signal transduction (16), our findings allow us to propose a new hypothesis: Th17 cell differentiation is regulated by a pathway that is distinct from the IFNγ signaling pathway. Therefore, we suggest that T-bet expression either directly or indirectly suppresses Th17 cell differentiation via an IFNγ-independent mechanism.

Tbx21 expression was significantly higher in T-bet–Tg mice as compared with B6 mice, and FACS analysis of CII-reactive CD4+ T cells revealed a significantly higher percentage of T-bet+ cells among the CD4+ T cell subset in T-bet–Tg mice. While there was no significant difference in the percentage of RORγt+ cells among the CD4+ T cell subset in T-bet–Tg mice as compared with B6 mice, *Rorc* expression was down-regulated on CII-reactive CD4+ T cells in T-bet–Tg mice. In the case of CD4+ T cells under

conditions favoring Th17 cell differentiation, RORγt expression on CD4+ T cells from T-bet–Tg mice was lower than that on cells from B6 mice. Interestingly, most of the RORγt+ cells also expressed T-bet in T-bet–Tg mice, and the proportion of IL-17–producing RORγt+ T cells in the CD4+ cell subset was lower in T-bet–Tg mice than in B6 mice. These findings support the notion that overexpression of T-bet not only suppresses RORγt expression on CD4+ T cells, but also inhibits the production of IL-17 from RORγt+ T cells.

Previous studies showed that RORγt expression is positively regulated by several transcription factors, such as runt-related transcription factor 1 (RUNX-1), interferon regulatory factor 4, and STAT-3 (26–28). Lazarevic et al (29) recently reported that T-bet prevented RUNX-1–mediated activation of the gene encoding RORγt, followed by the suppression of Th17 cell differentiation. In addition to direct promotion of RORγt expression, RUNX-1 also acts as a coactivator, together with RORγt, and induces the expression of *Il17a* and *Il17f* (26); therefore, T-bet inhibits IL-17 production by RORγt+ cells induced by RUNX-1 (29). Although further studies will be required to identify the effect of T-bet overexpression on the function of RUNX-1, it might be associated with the suppression of Th17 cell differentiation that was observed in the T-bet–Tg mice.

In conclusion, our results demonstrated that overexpression of T-bet in T cells suppressed the development of autoimmune arthritis. The regulatory mechanism of CIA might involve dysfunction of CII-reactive Th17 cell differentiation by overexpression of T-bet via IFNγ-independent pathways. These findings should enhance our understanding of the pathogenesis of autoimmune arthritis and help in the development of new therapies for RA.

ACKNOWLEDGMENT

We thank Dr. F. G. Issa for critical reading of the manuscript.

AUTHOR CONTRIBUTIONS

All authors were involved in drafting the article or revising it critically for important intellectual content, and all authors approved the final version to be published. Dr. Sumida had full access to all of the data in the study and takes responsibility for the integrity of the data and the accuracy of the data analysis.

Study conception and design. Sugihara, Hayashi, Yoh, Takahashi, Matsumoto, Sumida.

Acquisition of data. Kondo, Yao, Tahara.

Analysis and interpretation of data. Kondo, Iizuka, Wakamatsu, Tsuboi, Matsumoto.

REFERENCES

1. Miltenburg AM, van Laar JM, de Kuiper R, Daha MR, Breedveld FC. T cells cloned from human rheumatoid synovial membrane functionally represent the Th 1 subset. Scand J Immunol 1992;35: 603–10.
2. Iwanami K, Matsumoto I, Tanaka-Watanabe Y, Inoue A, Mihara M, Ohsugi Y, et al. Crucial role of the interleukin-6/interleukin-17 cytokine axis in the induction of arthritis by glucose-6-phosphate isomerase. Arthritis Rheum 2008;58:754–63.
3. Nakae S, Nambu A, Sudo K, Iwakura Y. Suppression of immune induction of collagen-induced arthritis in IL-17-deficient mice. J Immunol 2003;171:6173–7.
4. Chu CQ, Swart D, Alcorn D, Tocker J, Elkon KB. Interferon-γ regulates susceptibility to collagen-induced arthritis through suppression of interleukin-17. Arthritis Rheum 2007;56:1145–51.
5. Geboes L, De Klerck B, Van Balen M, Kelchtermans H, Mitera T, Boon L, et al. Freund's complete adjuvant induces arthritis in mice lacking a functional interferon-γ receptor by triggering tumor necrosis factor α–driven osteoclastogenesis. Arthritis Rheum 2007;56:2595–607.
6. Chabaud M, Durand JM, Buchs N, Fossiez F, Page G, Frappart L, et al. Human interleukin-17: a T cell–derived proinflammatory cytokine produced by the rheumatoid synovium. Arthritis Rheum 1999;42:963–70.
7. Shen H, Goodall JC, Gaston JS. Frequency and phenotype of peripheral blood Th17 cells in ankylosing spondylitis and rheumatoid arthritis. Arthritis Rheum 2009;60:1647–56.
8. Szabo SJ, Kim ST, Costa GL, Zhang X, Fathman CG, Glimcher LH. A novel transcription factor, T-bet, directs Th1 lineage commitment. Cell 2000;100:655–69.
9. Afkarian M, Sedy JR, Yang J, Jacobson NG, Cereb N, Yang SY, et al. T-bet is a STAT1-induced regulator of IL-12R expression in naive $CD4^+$ T cells. Nat Immunol 2002;57:549–57.
10. Ivanov II, McKenzie BS, Zhou L, Tadokoro CE, Lepelley A, Lafaille JJ, et al. The orphan nuclear receptor RORγt directs the differentiation program of proinflammatory IL-17+ T helper cells. Cell 2006;126:1121–33.
11. Hawng ES, Szabo SJ, Schwartzberg PL, Glimcher LH. T helper cell fate specified by kinase-mediated interaction of T-bet with GATA-3. Science 2005;307:430–3.
12. Zhou L, Lopes JE, Chong MM, Ivanov II, Min R, Victora GD, et al. TGF-β-induced Foxp3 inhibits T_H17 cell differentiation by antagonizing RORγt function. Nature 2008;453:236–41.
13. Buttgereit F, Zhou H, Kalak R, Gaber T, Spies CM, Huscher D, et al. Transgenic disruption of glucocorticoid signaling in mature osteoblasts and osteocytes attenuates K/BxN mouse serum–induced arthritis in vivo. Arthritis Rheum 2009;60:1998–2007.
14. Ishizaki K, Yamada A, Yoh K, Nakano T, Shimohata H, Maeda A, et al. Th1 and type 1 cytotoxic T cells dominate responses in T-bet overexpression transgenic mice that develop contact dermatitis. J Immunol 2007;178:605–12.
15. Cho YG, Cho ML, Min SY, Kim HY. Type II collagen autoimmunity in a model of human rheumatoid arthritis. Autoimmun Rev 2007;7:65–70.
16. Tanaka K, Ichiyama K, Hashimoto M, Yoshida H, Takimoto T, Takaesu G, et al. Loss of suppressor of cytokine signaling 1 in helper T cells leads to defective Th17 differentiation by enhancing antagonistic effects of IFN-γ on STAT3 and Smads. J Immunol 2008;180:3746–56.
17. Kiwamoto T, Ishii Y, Morishima Y, Yoh K, Maeda A, Ishizaki K, et al. Transcription factor T-bet and GATA-3 regulate development of airway remodeling. Am J Respir Crit Care Med 2006;174: 142–51.
18. Shimohata H, Yamada A, Yoh K, Ishizaki K, Morito N, Yamagata K, et al. Overexpression of T-bet in T cells accelerates auto-

immune glomerulonephritis in mice with a dominant Th1 background. J Nephrol 2009;22:123–9.
19. Rangachari M, Mauermann N, Marty RR, Dirnhofer S, Kurrer MO, Komnenovic V, et al. T-bet negatively regulates autoimmune myocarditis by suppressing local production of interleukin 17. J Exp Med 2006;203:2009–19.
20. Nath N, Prasad R, Giri S, Singh AK, Singh I. T-bet is essential for the progression of experimental autoimmune encephalomyelitis. Immunology 2006;118:384–91.
21. Yang Y, Weiner J, Liu Y, Smith AJ, Huss DJ, Winger R, et al. T-bet is essential for encephalitogenicity of both Th1 and Th17 cells. J Exp Med 2009;206:1549–64.
22. Neurath MF, Weigmann B, Finotto S, Glickman J, Nieuwenhuis E, Iijima H, et al. The transcription factor T-bet regulates mucosal T cell activation in experimental colitis and Crohn's disease. J Exp Med 2002;195:1129–43.
23. Juedes AE, Rodrigo E, Togher L, Glimcher LH, von Herrath MG. T-bet controls autoaggressive CD8 lymphocyte responses in type 1 diabetes. J Exp Med 2004;199:1153–62.
24. Hosoya T, Kuroha T, Moriguchi T, Cummings D, Maillard I, Lim KC, et al. GATA-3 is required for early T lineage progenitor development. J Exp Med 2009;206:2987–3000.
25. Shi G, Wang Z, Jin H, Chen YW, Wang Q, Qian Y. Phenotype switching by inflammation-inducing polarized Th17 cells, but not by Th1 cells. J Immunol 2008;181:7205–13.
26. Zhang F, Meng G, Strober W. Interactions among the transcription factors Runx1, RORγt and Foxp3 regulate the differentiation of interleukin 17–producing T cells. Nat Immunol 2008;9:1297–306.
27. Brustle A, Heink S, Huber M, Rosenplanter C, Stadelmann C, Yu P, et al. The development of inflammatory T_H-17 cells requires interferon-regulatory factor 4. Nat Immunol 2007;8:958–66.
28. Durant L, Watford WT, Ramos HL, Laurence A, Vahedi G, Wei L, et al. Diverse targets of the transcription factor STAT3 contribute to T cell pathogenicity and homeostasis. Immunity 2010;32:605–15.
29. Lazarevic V, Chen X, Shim JH, Hwang ES, Jang E, Bolm AN, et al. T-bet represses T_H17 differentiation by preventing Runx1-mediated activation of the gene encoding RORγt. Nat Immunol 2011;12:96–104.

ARTHRITIS & RHEUMATISM
Vol. 64, No. 12, December 2012, pp 3877–3885
DOI 10.1002/art.34666

Murine Tumor Necrosis Factor α–Induced Adipose-Related Protein (Tumor Necrosis Factor α–Induced Protein 9) Deficiency Leads to Arthritis via Interleukin-6 Overproduction With Enhanced NF-κB, STAT-3 Signaling, and Dysregulated Apoptosis of Macrophages

Asuka Inoue,[1] Isao Matsumoto,[1] Yoko Tanaka,[1] Naoto Umeda,[1] Yuki Tanaka,[1] Masahiko Mihara,[2] Satoru Takahashi,[1] and Takayuki Sumida[1]

Objective. **To elucidate the role of tumor necrosis factor α–induced adipose-related protein (TIARP; or tumor necrosis factor α–induced protein 9 [TNFAIP-9]) in the development and pathogenesis of arthritis.**

Methods. **We generated TIARP-deficient ($TIARP^{-/-}$) mice and investigated several organs in aged mice. Peritoneal macrophages were collected and cultured with lipopolysaccharide (LPS) and TNFα, and then the production of cytokines and subsequent NF-κB signal transduction were analyzed. We also examined the susceptibility of young $TIARP^{-/-}$ mice to collagen-induced arthritis (CIA). Draining lymph nodes and splenocytes were isolated and cultured, and serum levels of anti–type II collagen (anti-CII) antibodies, interleukin-6 (IL-6), and TNFα on day 60 were measured. We further investigated the effects of anti–IL-6 receptor monoclonal antibody (mAb) on the development of arthritis in $TIARP^{-/-}$ mice. IL-6/STAT-3 signaling was also analyzed using $TIARP^{-/-}$ macrophages.**

Results. **$TIARP^{-/-}$ mice developed spontaneous enthesitis and synovitis, had high serum levels of IL-6, had increased CD11b+ cell counts in the spleen, and showed enhanced LPS- and TNFα-induced IL-6 expression in macrophages. Sustained degradation of IκBα with dysregulated apoptosis was also noted in $TIARP^{-/-}$ macrophages. CIA was clearly exacerbated in $TIARP^{-/-}$ mice, accompanied by marked neutrophil and macrophage infiltration in joints. The levels of anti-CII antibodies in serum were unchanged, whereas autoreactive Th1 cell and Th17 cell responses were higher in $TIARP^{-/-}$ mice. Treatment with anti–IL-6 receptor mAb prevented the development of CIA in $TIARP^{-/-}$ mice, and $TIARP^{-/-}$ macrophages showed increased IL-6–induced STAT-3 phosphorylation.**

Conclusion. **These findings suggest that TIARP acts as a negative regulator of arthritis by suppressing IL-6 production, its signaling and TNFα-induced NF-κB signaling, resulting in enhanced apoptosis in macrophages.**

The prognosis in patients with rheumatoid arthritis (RA) has improved significantly with the recent availability of biologic agents that target tumor necrosis factor α (TNFα) and interleukin-6 (IL-6) (1,2). However, the exact mechanisms of action of these agents remain largely unknown. Glucose-6-phosphate isomerase (GPI) was first identified as an arthritogenic target in K/BxN mice (3), and GPI immunization of DBA/1 mice was shown to lead to arthritis (GPI-induced arthritis) (4). Studies in GPI-induced arthritis showed clear therapeutic benefits of treatment with TNFα and IL-6 antagonists (5,6), suggesting its suitability for analyzing the mechanisms of action of these agents in RA.

Using GeneChip analysis, we previously demon-

Supported in part by a grant from the Japanese Ministry of Science and Culture to Drs. Matsumoto and Sumida.

[1]Asuka Inoue, PhD, Isao Matsumoto, MD, PhD, Yoko Tanaka, PhD, Naoto Umeda, MD, Yuki Tanaka, MS, Satoru Takahashi, MD, PhD, Takayuki Sumida, MD, PhD: Graduate School of Comprehensive Human Sciences, University of Tsukuba, Tsukuba, Japan; [2]Masahiko Mihara, PhD: Chugai Pharmaceutical Company, Gotemba, Japan.

Dr. Matsumoto has received a research grant from Bristol-Myers Squibb.

Address correspondence to Isao Matsumoto, MD, PhD, Division of Clinical Immunology, Doctoral Program in Clinical Science, Graduate School of Comprehensive Human Sciences, University of Tsukuba, 1-1-1 Tennodai, Tsukuba 305-8575, Japan. E-mail: ismatsu@md.tsukuba.ac.jp.

Submitted for publication March 1, 2012; accepted in revised form August 2, 2012.

strated the up-regulation of TNFα-induced adipose-related protein (TIARP) in GPI-induced arthritis (7), as well as in CD11b+ splenocytes and joints of mice. Human TIARP counterparts, such as 6-transmembrane epithelial antigen of prostate 4 (STEAP-4), were also found to be highly expressed in peripheral blood monocytes, neutrophils, and synovial CD68+ cells from patients with RA (7,8). However, the role of TIARP in the pathogenesis of autoimmune arthritis remains to be confirmed.

In this study, we found that TIARP-deficient ($TIARP^{-/-}$) mice develop spontaneous enthesitis and synovitis, with high numbers of macrophages and elevated IL-6 expression. $TIARP^{-/-}$ macrophages showed enhanced NF-κB signaling, with dysregulated TNFα-induced apoptosis, and showed increased IL-6–induced STAT-3 phosphorylation. Moreover, the development of collagen-induced arthritis (CIA) was markedly exacerbated in $TIARP^{-/-}$ mice, suggesting that TIARP may provide new insights into the pathogenesis of arthritis as a negative regulator.

MATERIALS AND METHODS

Mice. The $TIARP^{-/-}$ mouse line was generated by homologous recombination in embryonic stem cells from mice of the C57BL/6 (B6) background. A conditional targeting vector for the TIARP gene was designed to delete exon 2, with a DNA fragment containing a loxP-flanked neomycin resistance gene and herpes simplex virus thymidine kinase gene (illustration available upon request from the corresponding author). All mice were maintained under specific pathogen–free conditions in an environmentally controlled clean room at the University of Tsukuba. All animal experiments were approved by the institutional committee and were conducted in accordance with the institutional ethics guidelines.

Histopathologic examination. When the mice were 12 months of age, we removed the primary organs and tissues, including the ankle joints, lungs, salivary glands, white adipose tissue, liver, thymus, spleen, inguinal lymph nodes, stomach, small intestine, large intestine, kidneys, and reproductive organs, for histopathologic examination. Tissues were fixed in neutralized 10% formalin, and the joints of the right hind paw were decalcified in 10% formic acid and embedded in paraffin. We stained 4-mm serial sections with hematoxylin and eosin or toluidine blue and scored the tissues for histologic changes. Sections were graded on a scale of 0–5, where 0 = normal and 5 = severe. One point was given for the presence of each of the following features of enthesitis: inflammatory cell infiltration, entheseal fibroblast-like cell proliferation, cartilage formation, bone formation, and ankylosis. The same system was used to grade synovitis, with 1 point given for each of the following features: inflammatory cell infiltration, synovial hyperplasia, pannus formation, cartilage degradation, and bone degradation.

For immunohistochemical staining, the sections were incubated overnight at 4°C with rat anti–Gr-1 or anti-F4/80. The signals were detected with Alexa 488–conjugated anti-rat IgG. Nuclei were counterstained with DAPI. The sections were examined under fluorescence microscopy (Keyence).

Flow cytometric analysis. For flow cytometry, cells were stained with fluorescein isothiocyanate (FITC)–, phycoerythrin-, PerCP-, or allophycocyanin-conjugated monoclonal antibodies (mAb). Rat mAb to mouse CD3, CD4, CD8, CD11b, Gr-1, F4/80, CD11c, IL-17, and interferon-γ (IFNγ) were purchased from BioLegend, and rat mAb to mouse FoxP3 was purchased from eBioscience. Apoptosis was detected by staining with propidium iodide and FITC-conjugated annexin V (BioLegend). We performed cell surface staining according to standard techniques. Stained cells were identified with a FACSCalibur cytometer (Becton Dickinson) using FlowJo software (Tree Star).

Real-time quantitative polymerase chain reaction (PCR) analysis. We isolated total RNA from splenocytes and ankle joints by the Isogen (Nippon Gene) extraction method according to the instructions provided by the manufacturer. We performed real-time quantitative PCR as described previously (7) using a TaqMan gene expression assay (Applied Biosystems) and the following probes: TIARP (Mm00475402_m1), TNFα (Mm00443258_m1), IL-6 (Mm00446190_m1), CXCL2 (Mm00436450_m1), matrix metalloproteinase 3 (MMP-3) (Mm00440295_m1), RANKL (Mm00441906_m1), and GAPDH (Mm99999915_g1). Real-time quantitative PCR was carried out using an ABI 7500 analyzer (Applied Biosystems). Analysis of post-PCR melting curves confirmed the specificity of the single-target amplification. We determined the expression of each gene relative to GAPDH.

Thioglycolate-elicited macrophages. Mice were injected intraperitoneally with 2 ml of 3% thioglycolate. After 3 days, mice were euthanized and peritoneal macrophages were collected by phosphate buffered saline (PBS) lavage. Cells were incubated for the indicated durations in the presence or absence of 100 ng/ml of TNFα, 100 ng/ml of lipopolysaccharide (LPS), or 10 ng/ml of IL-6.

Immunoblotting. Cells were lysed in 0.5% Nonidet P40, 5 m*M* $MgCl_2$, 50 m*M* Tris HCl (pH 7.4), and 2 m*M* phenylmethylsulfonyl fluoride. Equal amounts of protein were subjected to immunoblotting using antibodies to IκBα, phospho-STAT-3, STAT-3, and suppressor of cytokine signaling 3 (SOCS-3), as well as phospho-ERK-1/2, ERK-1/2, caspase 3, cleaved caspase 3 antibodies (Cell Signaling Technology), and anti-actin antibodies (Bio-Rad). Densitometric analysis was carried out using an ImageQuant LAS 4000 densitometer (GE Healthcare).

Collagen-induced arthritis. CIA was induced in mice of the B6 background. We immunized 8–12-week-old mice intradermally at several sites at the base of the tail with 100 μl of 200 μg chicken type II collagen (CII; Sigma) emulsified in Freund's incomplete adjuvant (Difco) and containing 5 mg/ml of heat-killed *Mycobacterium tuberculosis* (H37Ra; Difco). According to the usual immunization schedule, mice were rechallenged with CII and Freund's complete adjuvant on day 21 after the primary immunization. Arthritis was assessed every other day by examining each joint for swelling and redness. Arthritis severity was graded on a scale of 0–3 in each paw. The clinical score for each mouse was the sum of the scores for the 4 paws (maximum score 12).

Enzyme-linked immunosorbent assay (ELISA). Single-cell suspensions were prepared from the spleens and lymph nodes of wild-type (WT) and $TIARP^{-/-}$ mice. Cells were

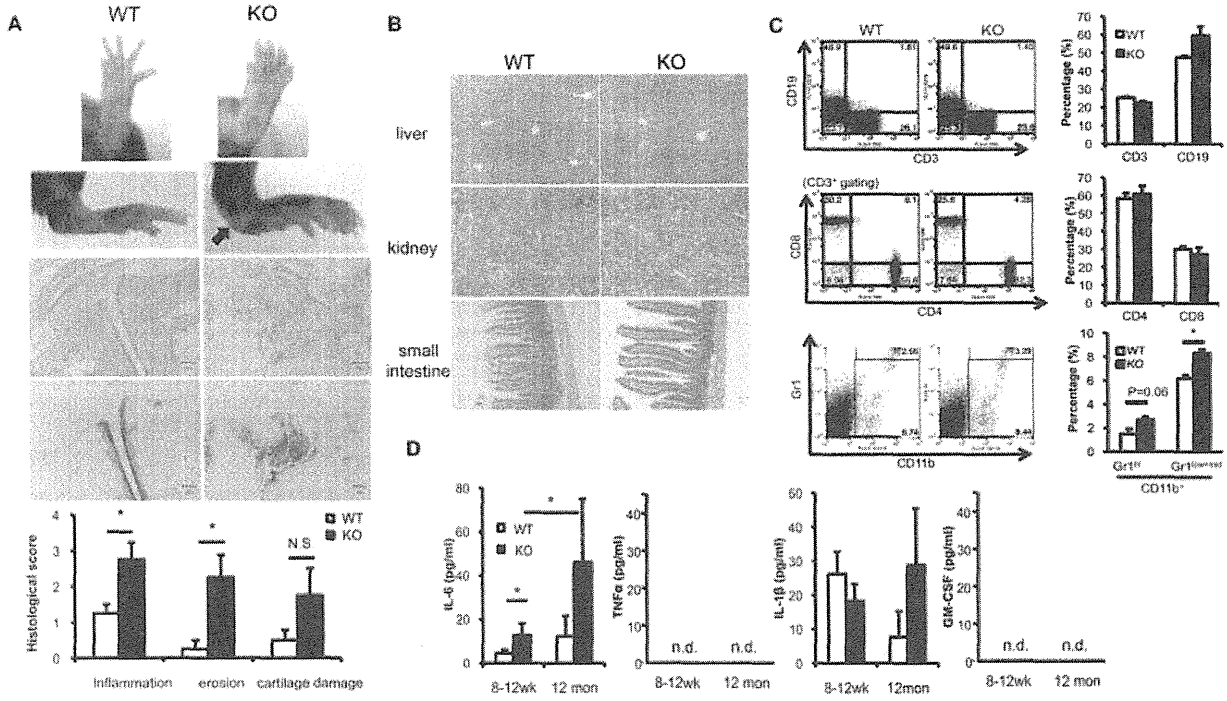

Figure 1. Development of arthritis in aged tumor necrosis factor α–induced adipose-related protein (TIARP)–knockout (KO) mice, with increased numbers of macrophages and overproduction of interleukin-6 (IL-6) as compared to wild-type (WT) mice. **A,** Macroscopic (top) and microscopic (middle) appearance of the ankle joints of 12-month-old WT and TIARP$^{-/-}$ mice, along with histology scores (bottom). **Arrow** in the ankle joint photograph indicates inflammatory changes. Photomicrographs of hematoxylin and eosin (H&E)–stained (top) and toluidine blue–stained (bottom) sections of the ankle joints demonstrate the histopathologic changes. Original magnification × 20. Histology scores for inflammation, erosion, and cartilage damage were higher in the TIARP$^{-/-}$ mice. Values are the mean ± SEM of 2 independent experiments (n = 5 mice per group per experiment). * = $P < 0.05$, by Student's *t*-test. NS = not significant. **B,** Histologic assessment of H&E-stained sections of liver, kidney, and small intestine from WT and TIARP$^{-/-}$ mice. Original magnification × 20. **C,** Flow cytometry of splenocytes from 12-month-old WT and TIARP$^{-/-}$ mice (left) and percentages of the indicated cell subsets (right). Cells were stained with a combination of antibodies and analyzed as described in Materials and Methods. Values in each compartment are the percentages of cells. The percentages of splenic CD11b+Gr-1^{high} cells (neutrophils) and CD11b+Gr-1$^{low/intermediate}$ cells (macrophages) were determined. Values are the mean ± SEM of 2 independent experiments (n = 5 mice per group per experiment). * = $P < 0.05$, by Student's *t*-test. **D,** Serum concentrations of IL-6, tumor necrosis factor α (TNFα), IL-1β, and granulocyte–macrophage colony-stimulating factor (GM-CSF) in 8–12-week-old and 12-month-old mice. Values are the mean ± SEM of 2 independent experiments (n = 5 mice per group per experiment). * = $P < 0.05$, by Student's *t*-test. ND = not detected.

cultured for 72 hours at 37°C in an atmosphere containing 5% CO_2, and supernatants were collected. Levels of IL-6 and TNFα in the cell culture supernatants were measured using ELISA kits (R&D Systems). Serum samples were collected on days 30 and 60 from arthritic WT and TIARP$^{-/-}$ mice, and serum levels of TNFα, IL-6, IL-1β, and granulocyte–macrophage colony-stimulating factor (GM-CSF) were measured with ELISA kits (R&D Systems). Serum levels of anti-CII antibodies were also analyzed for CII-specific IgG antibodies by ELISA. All serum samples were diluted 1:3,000 in PBS prior to ELISA.

Treatment of arthritis with anticytokine antibodies. For IL-6 neutralization, mice were injected intraperitoneally with 2 mg of MR16-1 (a rat IgG1 mAb against murine IL-6 receptor [IL-6R]) or control IgG (purified from the serum of nonimmunized rats) on day 21 after induction of CIA. MR16-1 was a gift from Chugai Pharmaceutical, and control IgG was purchased from Jackson ImmunoResearch. To neutralize TNFα, mice were injected intraperitoneally with 100 μg of neutralizing antibody or isotype control on day 21. Anti-TNFα mAb MP6-XT3 (IgG1, rat) and IgG1 isotype control (rat) were purchased from eBioscience.

Statistical analysis. In the CIA experiments, disease incidence was evaluated with the chi-square test and the severity score by the Mann-Whitney U test. Student's *t*-test was used for the evaluation of all other results. *P* values less than 0.05 were considered significant.

RESULTS

Spontaneous development of destructive arthritis, with increased numbers of macrophages and high serum levels of IL-6, in TIARP-deficient mice. TIARP$^{-/-}$ mice were generated to further investigate

Table 1. Abnormal clinical and histologic features in aged (12-month-old) male TIARP$^{-/-}$ mice as compared with their wild-type littermates

Characteristic	Wild-type mice (n = 13)	Knockout mice (n = 13)
Clinical features		
Incidence of arthritis, no. (%)	0 (0.0)	10 (76.9)*
Mean ± SEM clinical score	0.00 ± 0.00	2.25 ± 0.62*
Histologic score		
Inflammation, mean ± SEM	1.25 ± 0.25	2.75 ± 0.48†
Erosions, mean ± SEM	0.25 ± 0.25	2.25 ± 0.63†
Cartilage damage, mean ± SEM	0.50 ± 0.29	1.75 ± 0.75†

* $P < 0.005$.
† $P < 0.05$.

the function of TIARP in arthritis. To do this, we used homologous recombination in embryonic stem cells derived from B6 mice to produce a line of mice carrying a defective TIARP gene. In the homozygous state, these mice carry a mutant allele with exon 2 deleted (data available upon request from the corresponding author). The expression of the mature TIARP gene and protein in splenocytes, peritoneal macrophages, and synoviocytes (data not shown) could not be detected by real-time quantitative PCR and Western blotting.

We then tested whether deletion of the TIARP gene could directly induce organ autoimmunity. We found that 76.9% of the deficient mice developed joint abnormalities by 12 months of age (Figure 1A and Table 1). Furthermore, marked enthesopathy and weak synovitis with joint destruction were observed in these TIARP$^{-/-}$ mice (Figure 1A). These findings were confirmed by histologic scoring of inflammation and erosion (Figure 1A). We also screened several other organs isolated from 20-week-old and 12-month-old mice. The murine white adipose tissues showed weak cell infiltration, confirming the findings of Wellen et al (9), although there was no significant cell infiltration or damage in the liver, kidney, or small intestine (Figure 1B) or in the white adipose tissue, large intestine, or other organs (data available upon request from the corresponding author).

Immune cell development and function in TIARP$^{-/-}$ mice were investigated next. The involvement of acquired immune cells in the spleen (Figure 1C) and in the thymus and mesenteric and inguinal lymph nodes (LNs) (data not shown) in TIARP$^{-/-}$ mice was almost comparable to WT mice. Because TIARP is highly expressed in CD11b+ cells during GPI-induced arthritis (7), we screened the spleens of TIARP$^{-/-}$ mice and found significantly high numbers of CD11b+

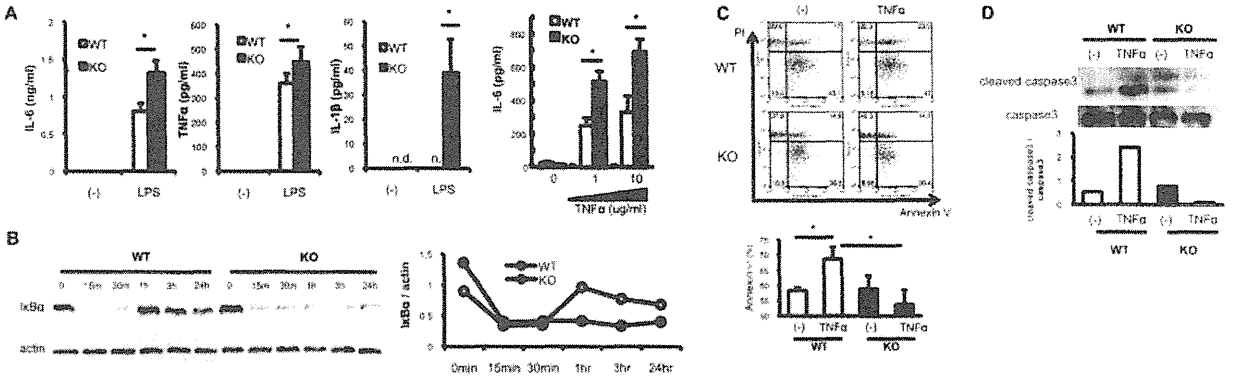

Figure 2. Enhanced responsiveness of macrophages from TIARP$^{-/-}$ mice to lipopolysaccharide (LPS) and TNFα. **A,** Levels of IL-6, TNFα, and IL-1β in culture supernatants, as determined by enzyme-linked immunosorbent assay. Thioglycolate-elicited macrophages from TIARP$^{-/-}$ and WT mice were cultured for 12 hours in the presence or absence of LPS or were cultured for 96 hours in the presence or absence of 1 μg/ml or 10 μg/ml of TNFα. Values are the mean ± SEM of 3 independent experiments (n = 5 mice per group per experiment). * = $P < 0.05$. **B,** Levels of IκBα in extracts of thioglycolate-elicited macrophages from TIARP$^{-/-}$ and WT mice, as determined by immunoblot analysis. Cells were incubated with 100 ng/ml of TNFα for the indicated times, and immunoblotting was performed, as shown at the left. Actin was used as a loading control. Results of densitometric quantification of IκBα levels are shown at the right. Values are the mean. **C,** Flow cytometry of apoptotic cell populations in macrophages left unstimulated or stimulated for 24 hours with TNFα, as detected by propidium iodide and annexin V staining. Percentages of annexin V+ cells are shown at the bottom. Values are the mean ± SEM of 2 independent experiments (n = 5 mice per group per experiment). * = $P < 0.05$. **D,** Analysis of caspase 3 and cleaved caspase 3 in macrophages. Thioglycolate-elicited macrophages were treated with 100 ng/ml of TNFα, and total cell lysates were immunoblotted with antibodies to cleaved caspase 3 (bands at 17 kd and 19 kd) or caspase 3, as shown at the top. Results of densitometric quantification of the ratio of cleaved caspase 3 to caspase 3 are shown at the bottom. Values are the mean. See Figure 1 for other definitions.

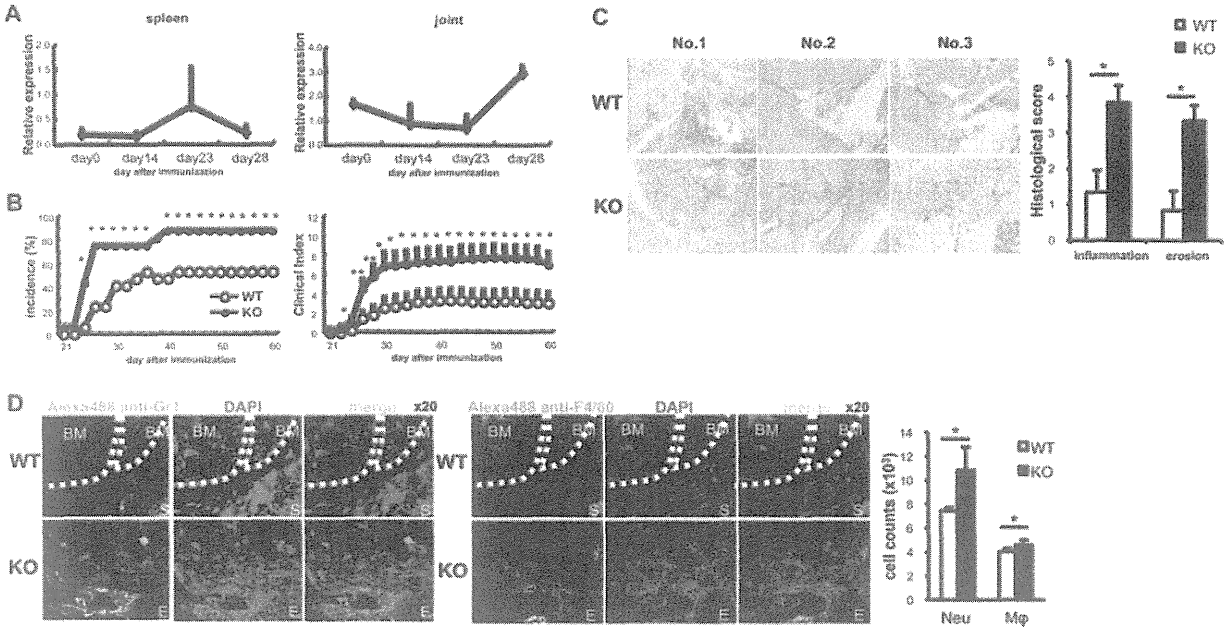

Figure 3. Exacerbation of collagen-induced arthritis (CIA), with marked infiltration of neutrophils and macrophages, in TIARP$^{-/-}$ mice. **A**, Expression of mRNA for TIARP in the spleen and joints obtained on the indicated days from TIARP$^{-/-}$ and WT mice with CIA. Values are the mean ± SEM of 3 independent experiments (n = 5 mice per group per experiment). **B**, Arthritis incidence and severity scores in TIARP$^{-/-}$ and WT mice with CIA. Values are the mean ± SEM of 3 independent experiments (n = 16–17 mice per group per experiment). * = $P < 0.05$. **C**, Histopathologic analysis of joint sections obtained on day 60 after immunization in 3 mice from each group. Original magnification × 20. Histopathology scores for inflammation and erosion are shown at the right. Values are the mean ± SEM of 2 independent experiments (n = 5 mice per group per experiment). * = $P < 0.05$. **D**, Immunofluorescence analysis of neutrophils and macrophages using anti–Gr-1 and anti-F4/80 monoclonal antibodies, respectively, in the bone marrow (BM), synovium (S), and exudate (E) of ankle joints obtained on day 60. Broken lines in the top panels of the photomicrographs indicate the surface of the articular cartilage. Original magnification × 20. Numbers of neutrophils and macrophages in the ankle joints as determined on day 60 are shown at the right. Values are the mean ± SEM of 2 independent experiments (n = 5 mice per group per experiment). * = $P < 0.05$. See Figure 1 for other definitions. Color figure can be viewed in the online issue, which is available at http://onlinelibrary.wiley.com/journal/10.1002/(ISSN)1529-0131.

Gr-1$^{low/intermediate}$ cells (confirmed by microscopy to be macrophages) (Figure 1C).

We next examined inflammatory cytokines in the TIARP$^{-/-}$ mice, since they are also key players in RA

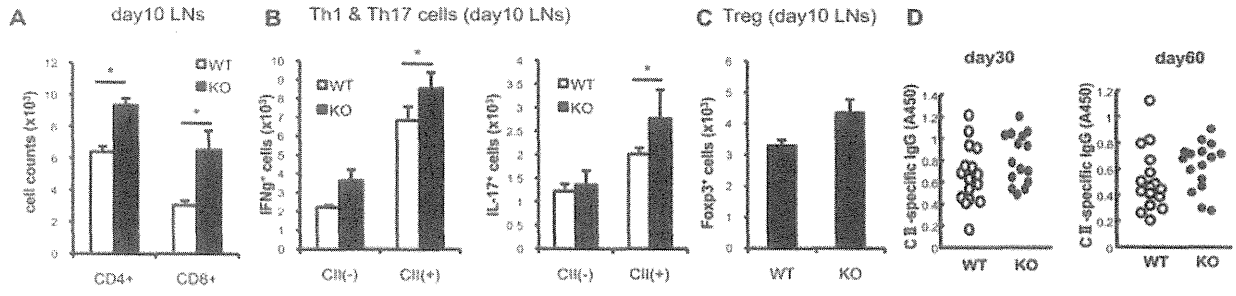

Figure 4. Enhanced type II collagen (CII)–specific Th1 cells and Th17 cells, with comparable amounts of anti-CII antibodies, in tumor necrosis factor α–induced adipose-related protein (TIARP)–knockout (KO) mice as compared to wild-type (WT) mice. **A**, Numbers of CD4+ and CD8+ cells in draining lymph nodes (LNs) obtained on day 10. Values are the mean ± SEM of 3 independent experiments (n = 5 mice per group per experiment). * = $P < 0.05$. **B** and **C**, Numbers of interferon-γ (IFNγ)–positive and interleukin-17 (IL-17)–positive cells (**B**) and numbers of FoxP3-positive Treg cells (**C**) in draining LNs obtained on day 10, as determined by flow cytometry, gating on CD3+CD4+ cells. Values are the mean ± SEM of 3 independent experiments (n = 5 mice per group per experiment). * = $P < 0.05$. **D**, Serum levels of CII-specific IgG in 16 WT mice and 17 TIARP$^{-/-}$ mice on day 30 and day 60 after immunization. Each symbol represents a single animal.

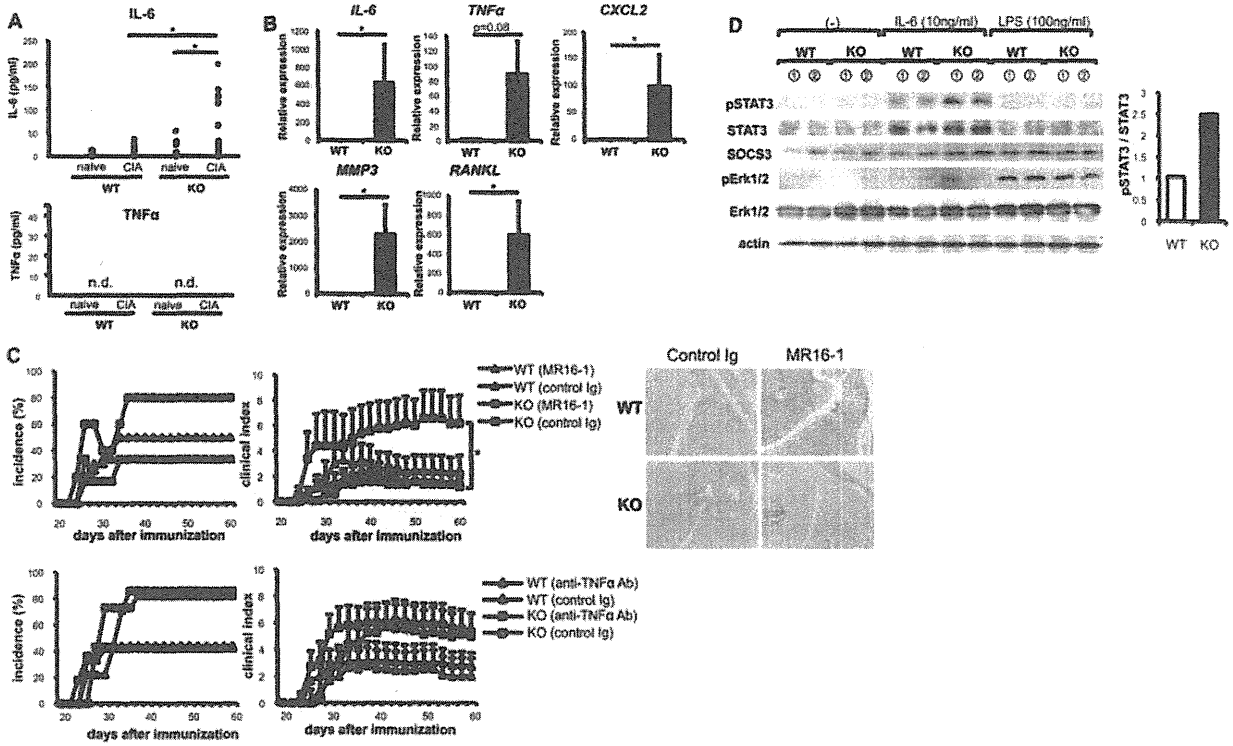

Figure 5. IL-6–triggered exacerbation of collagen-induced arthritis (CIA) in TIARP$^{-/-}$ mice. **A,** Serum levels of IL-6 (top) and TNFα (bottom) on day 0 and day 60 after immunization in naive mice (n = 10–12 mice per group per experiment) and mice with CIA (n = 16 WT mice and n = 17 TIARP$^{-/-}$ mice). Each symbol represents a single animal. **B,** Expression of IL-6, TNFα, CXCL2, matrix metalloproteinase 3 (MMP-3), and RANKL genes in ankle joints obtained on day 60, as determined by real-time polymerase chain reaction analysis. Values are the mean ± SEM of 2 independent experiments (n = 5 mice per group per experiment). * = $P < 0.05$. **C,** Arthritis incidence and severity scores on day 21 in mice treated with 2 mg of anti–IL-6 receptor (anti–IL-6R) monoclonal antibody (mAb; MR16-1) (top) or with 100 μg of anti-TNFα mAb (bottom). Values are the mean ± SEM. * = $P < 0.05$. Histopathologic analysis of ankle joint sections obtained on day 60 after immunization following treatment with control Ig or with MR16-1 mAb is shown at the right. Original magnification × 20. **D,** Levels of pSTAT-3, STAT-3, SOCS-3, pERK-1/2, and ERK-1/2 in cell lysates of thioglycolate-elicited macrophages from TIARP$^{-/-}$ and WT mice (n = 2 mice per group), as determined by immunoblot analysis. Cells were incubated for 1 hour in the absence or presence of 10 ng/ml of IL-6 or 100 ng/ml of lipopolysaccharide (LPS). Actin was used as a loading control. Results of densitometric quantification of the ratio of pSTAT-3 to STAT-3 are shown at the right. Values are the mean. See Figure 1 for other definitions. Color figure can be viewed in the online issue, which is available at http://onlinelibrary.wiley.com/journal/10.1002/(ISSN)1529-0131.

and are functionally linked to TIARP (10–12). Serum levels of IL-6 were higher in TIARP$^{-/-}$ mice than in WT mice irrespective of age, whereas no TNFα or GM-CSF was detected, and IL-1β levels were similar in WT and TIARP$^{-/-}$ mice (Figure 1D).

Taken together, these findings suggested that TIARP$^{-/-}$ mice develop spontaneous enthesopathy and synovitis, with elevated numbers of macrophages and elevated levels of IL-6, which suggest a pivotal role of macrophages.

Increased response to LPS and TNFα, sustained degradation of IκBα, and resistance to TNFα-induced apoptosis in macrophages from TIARP$^{-/-}$ mice. Next, we focused on CD11b+ cells, based on the dominant expression of TIARP in these cells in GPI-induced arthritis (7) and on the spontaneous aberrant accumulation of macrophages in TIARP$^{-/-}$ mice. Thioglycolate-activated peritoneal macrophages from TIARP$^{-/-}$ mice produced higher amounts of IL-6, TNFα, and IL-1β upon LPS stimulation (Figure 2A). Macrophages from TIARP$^{-/-}$ mice also produced higher amounts of IL-6 with TNFα stimulation (Figure 2A). Levels of IL-6Rα, TNF receptor type I (TNFRI), and TNFRII expression were similar in macrophages from TIARP$^{-/-}$ and WT mice (data not shown).

We then examined the role of TIARP in the NF-κB pathway and in apoptosis. Macrophages obtained from TIARP$^{-/-}$ mice and cultured with TNFα

showed sustained degradation of the NF-κB inhibitory molecule IκBα as compared to macrophages from WT mice (Figure 2B). Moreover, TNFα-induced apoptosis was increased in macrophages from WT mice, but was not significantly different in those from TIARP$^{-/-}$ mice (Figure 2C). Cleaved caspase 3 levels in the presence of TNFα were clearly diminished in macrophages from TIARP$^{-/-}$ mice as compared to WT mice (Figure 2D). Adding both TNFα and IL-6 induced proliferation in macrophages from TIARP$^{-/-}$ mice as compared to WT mice (data not shown).

Collectively, these results suggested that macrophages from TIARP$^{-/-}$ mice have a high level of response to TNFα due to a weak NF-κB-negative regulation and subsequent proliferation, with dysregulated apoptosis.

TIARP expression and fluctuation in mice with CIA. The direct pathogenic effect of TIARP in arthritis was explored using a model of CIA on a B6 background. We first examined TIARP fluctuations in CIA by screening for changes in TIARP expression in WT B6 mice. Real-time quantitative PCR showed up-regulated TIARP mRNA expression on day 23 in splenocytes from mice with CIA and on day 28 in the joints of the same mice, when the expression correlated with joint swelling (Figure 3A). These fluctuations resembled those seen in GPI-induced arthritis (7) and suggest that systemic up-regulation of TNFα and TIARP is involved in the early phases of the disease.

Exacerbation of CIA in TIARP$^{-/-}$ mice, with increased numbers of antigen-specific Th1 and Th17 cells in LNs, enhanced serum levels of IL-6, and infiltration of macrophages and neutrophils into the joints. Next, we induced CIA in 8–12-week-old TIARP$^{-/-}$ mice and found exacerbated disease incidence and severity in these mice as compared to the WT mice (Figure 3B). Histologic analysis of TIARP$^{-/-}$ mice with CIA showed marked cell infiltration, pannus formation, and bone erosion, as well as increased histology scores (Figure 3C). Immunohistochemical analysis of cells isolated from the mouse joints confirmed the dominance of neutrophil and macrophage infiltration in the joints of TIARP$^{-/-}$ mice (Figure 3D).

On day 10 after immunization with CII, the TIARP$^{-/-}$ mice had splenomegaly, and their CD4 and CD8 T cell counts were higher than those in WT mice (Figure 4A). In contrast, CD19+ cell counts were not different between WT mice and TIARP$^{-/-}$ mice (data not shown). We then screened T and B cell responses during CIA to investigate antigen-specific responses. The production of antigen-specific cytokines, such as IFNγ and IL-17, was significantly higher in draining LNs from TIARP$^{-/-}$ mice than in those from WT mice (Figure 4B), whereas the numbers of antigen-specific Treg cells (FoxP3+) were not significantly different (Figure 4C). Unexpectedly, the levels of antigen-specific anti-CII antibodies in TIARP$^{-/-}$ mice and WT mice were comparable on day 30 and on day 60 (Figure 4D).

Serum IL-6 levels on day 60 after immunization were also markedly increased in TIARP$^{-/-}$ mice compared to WT mice, whereas TNFα was not detected (Figure 5A). Gene expression analysis in mouse joints on day 60 showed higher levels of IL-6, CXCL2, MMP-3, and RANKL in TIARP$^{-/-}$ mice as compared to WT mice (Figure 5B).

Suppression of CIA in TIARP$^{-/-}$ mice by anti–IL-6R mAb. To further confirm the role of IL-6 in arthritis, IL-6 was inhibited after the onset of CIA (on day 21; this timing was generally not effective in WT mice [10]). As anticipated, injection of anti–IL-6R mAb significantly suppressed the incidence and progression of arthritis (Figure 5C, top), and histopathologic analysis on day 60 confirmed this effect (Figure 5C). In contrast, treatment with TNFα-neutralizing antibodies in TIARP$^{-/-}$ mice did not suppress the progression of arthritis (Figure 5C, bottom).

Enhanced signal in response to IL-6–induced STAT-3 expression in macrophages from TIARP$^{-/-}$ mice. To further investigate the role of IL-6 signal transduction in TIARP$^{-/-}$ mice, we also measured the expression of pSTAT-3, STAT-3, and SOCS-3 in macrophages. IL-6 stimulation induced STAT-3 and SOCS-3 expression in both groups of mice. However, only pSTAT-3 expression was enhanced in macrophages from TIARP$^{-/-}$ mice as compared to those from WT mice (Figure 5D). In addition, pERK-1/2 production was not changed.

DISCUSSION

In the present study, we demonstrated that TIARP$^{-/-}$ mice spontaneously develop enthesitis with synovitis and become susceptible to CIA. TIARP is detected during the course of adipocyte differentiation (11) and is also induced by IL-6 (12). TIARP-like proteins such as STEAP-4 are highly expressed in the bone marrow, placenta, and fetal liver (13). In murine hepatocytes, TNFα and IL-17 induce synergistic up-regulation of TIARP (14), and the TIARP gene is a direct target of phosphorylated STAT-3 (15). Recent reports suggest that the expression of 6-transmembrane protein of prostate 2 (STAMP-2)/STEAP-4 in CD14+ macrophages was significantly decreased in women with

metabolic syndrome and correlated with cardiovascular risk (16). The metabolic impact of TIARP has been confirmed in adipocytes from STAMP-2$^{-/-}$ mice (9), but its role in immunity and inflammation remains obscure (17).

Another TNF-induced protein, tumor necrosis factor α–induced protein 3 (TNFAIP-3), has become a particular focus because of its association with RA, as shown in genome-wide association studies (18,19). Matmati et al (20) recently revealed that mice deficient in myeloid-specific TNFAIP-3 spontaneously develop polyarthritis with increased numbers of CD11b+Gr-1+ cells and high levels of inflammatory cytokines (20). This arthritis is clearly dependent on IL-6 (and Toll-like receptor 4), but is independent of TNFα, T cells, and B cells. TIARP (TNFAIP-9) is expressed mainly in macrophages and neutrophils in mice (7) and in humans (8,16) with arthritic conditions, and TIARP$^{-/-}$ mice posses increased numbers of myeloid cells and cytokine dependency similar to that in the conditional TNFAIP-3–deficient mouse model. Thus, the expression of TNF-induced proteins of myeloid origin may be important for the regulation of arthritis via similar pathways.

We found significantly increased numbers of CD11b+Gr-1$^{low/intermediate}$ cells in mouse spleens; thus, we focused mainly on TIARP-dominant cells, such as macrophages, in this study. Stimulation with TNFα or with LPS enhanced the expression of IL-6 in macrophages from TIARP$^{-/-}$ mice. Following TNFα stimulation, sustained degradation of IκBα was noted, and subsequent proliferation with dysregulated apoptosis was seen in macrophages from TIARP$^{-/-}$ mice. Moreover, levels of IL-6–induced pSTAT-3 were also increased in TIARP$^{-/-}$ macrophages, as previously demonstrated in hepatocytes (15).

In addition to macrophages, CD11b+ neutrophils are another cellular source of TIARP/STEAP-4 (7,8). In TIARP$^{-/-}$ mice with CIA, overexpression of CXCL2 (the ligand of CXCR2) in joints was noted, with abundant recruitment of neutrophils. The numbers of CXCR2+ neutrophils were increased in TIARP$^{-/-}$ mice (data not shown), which probably enhanced the severity of the arthritis. In our previous study (8), we confirmed that STEAP-4 transfection of human neutrophils down-regulated their migration. It is possible that overproduction of IL-6 can also augment the adhesion of neutrophils (21).

CIA in the TIARP$^{-/-}$ mice was clearly exacerbated, and IL-6 overproduction was seen. Neutralization of IL-6 during the arthritis induction phase clearly suppressed the arthritis, suggesting a pivotal role of IL-6. The IL-6R-gp130^{F759} mutant mouse is a well-known model of spontaneous arthritis that develops around 12 months of age, with elevated numbers of Gr-1+ CD11b+ cells in LNs (22). In addition to Th17 cells, the importance of IL-6/STAT-3 signals in type I collagen fibroblasts was recently proven in this model (23). TIARP is weakly induced in T cells under arthritic conditions; however, their expression in joint fibroblasts has been confirmed in GPI-induced arthritis (7). STEAP-4 protein was also induced by TNFα in fibroblast-like synoviocytes (FLS), and transfection of STEAP-4 into FLS blocks inflammatory cytokines, such as IL-6 and IL-8, and induces apoptosis (24). Thus, TIARP can regulate innate immune cells and fibroblasts in joints to suppress inflammation and the proliferation that results in suppression of arthritis in an IL-6–related manner.

Taken together, the findings of this study implicate TIARP as a negative regulator of the arthritogenic process through the suppression of IL-6 production, NF-κB, STAT-3 signaling, and the induction of apoptosis. Moreover, systemic deletion of TIARP results in the specific development of RA-like pathology, suggesting that treatment with TIARP or with agents that stimulate TIARP may become an important option for the treatment of RA.

AUTHOR CONTRIBUTIONS

All authors were involved in drafting the article or revising it critically for important intellectual content, and all authors approved the final version to be published. Dr. Matsumoto had full access to all of the data in the study and takes responsibility for the integrity of the data and the accuracy of the data analysis.

Study conception and design. Inoue, Matsumoto, Sumida.

Acquisition of data. Inoue, Matsumoto, Yoko Tanaka, Umeda, Yuki Tanaka.

Analysis and interpretation of data. Inoue, Matsumoto, Mihara, Takahashi.

ADDITIONAL DISCLOSURE

Author Mihara is an employee of Chugai Pharmaceutical Company.

REFERENCES

1. Taylor PC, Feldmann M. Anti-TNF biologic agents: still the therapy of choice for rheumatoid arthritis. Nat Rev Rheumatol 2009;5:578–82.
2. Mima T, Nishimoto N. Clinical value of blocking IL-6 receptor. Curr Opin Rheumatol 2009;21:224–30.
3. Matsumoto I, Staub A, Benoist C, Mathis D. Arthritis provoked by linked T and B recognition of a glycolytic enzyme. Science 1999;286:1732–5.
4. Schubert D, Maier B, Morawietz L, Krenn V, Kamradt T. Immunization with glucose-6-phosphate isomerase induces T cell-dependent peripheral polyarthritis in genetically unaltered mice. J Immunol 2004;172:4503–9.
5. Matsumoto I, Zhang H, Yasukochi T, Iwanami K, Tanaka Y,

Inoue A, et al. Therapeutic effects of antibodies to tumor necrosis factor-α, interleukin-6 and cytotoxic T-lymphocyte antigen 4 immunoglobulin in mice with glucose-6-phosphate isomerase induced arthritis. Arthritis Res Ther 2008;10:R66.
6. Iwanami K, Matsumoto I, Tanaka-Watanabe Y, Inoue A, Mihara M, Ohsugi Y, et al. Crucial role of the interleukin-6/interleukin-17 cytokine axis in the induction of arthritis by glucose-6-phosphate isomerase. Arthritis Rheum 2008;58:754–63.
7. Inoue A, Matsumoto I, Tanaka Y, Iwanami K, Kanamori A, Ochiai N, et al. Tumor necrosis factor α-induced adipose-related protein expression in experimental arthritis and in rheumatoid arthritis. Arthritis Res Ther 2009;11:R118.
8. Tanaka Y, Matsumoto I, Iwanami K, Inoue A, Umeda N, Tanaka Y, et al. Six-transmembrane epithelial antigen of prostate 4 (STEAP4) is expressed on monocytes/neutrophils, and is regulated by TNF antagonist in patients with rheumatoid arthritis. Clin Exp Rheumatol 2012;30:99–102.
9. Wellen KE, Fucho R, Gregor MF, Furuhashi M, Morgan C, Lindstad T, et al. Coordinated regulation of nutrient and inflammatory response by STAMP2 is essential for metabolic homeostasis. Cell 2007;129:537–48.
10. Takagi N, Mihara M, Moriya Y, Nishimoto N, Yoshizaki K, Kishimoto T, et al. Blockage of interleukin-6 receptor ameliorates joint disease in murine collagen-induced arthritis. Arthritis Rheum 1998;41:2117–21.
11. Moldes M, Lasnier F, Gauthereau X, Klein C, Pairault J, Feve B, et al. Tumor necrosis factor-α-induced adipose-related protein (TIARP), a cell-surface protein that is highly induced by tumor necrosis factor-α and adipose conversion. J Biol Chem 2001;276:33938–46.
12. Fasshauer M, Kralisch M, Klier M, Lossner U, Bluher M, Chambaut-Guerin AM, et al. Interleukin-6 is a positive regulator of tumor necrosis factor α-induced adipose-related protein in 3T3-L1 adipocytes. FEBS Lett 2004;560:153–7.
13. Ohgami RS, Campagna DR, McDonald A, Fleming MD. The Steap proteins are metalloreductases. Blood 2006;108:1388–94.
14. Sparna T, Retey J, Schmich K, Albrecht U, Naumann K, Gretz N, et al. Genome-wide comparison between IL-17 and combined TNF-α/IL-17 induced genes in primary murine hepatocytes. BMC Genomics 2010;11:226.
15. Ramadoss P, Chiappini F, Biban M, Hollenberg AN. Regulation of hepatic six transmembrane epithelial antigen of prostate 4 (STEAP4) expression by STAT3 and CCAAT/enhancer-binding protein α. J Biol Chem 2010;285:16453–66.
16. Wang ZH, Zhang W, Gong HP, Guo ZX, Zhao J, Shang YY, et al. Expression of STAMP2 in monocytes associates with cardiovascular alterations. Eur J Clin Invest 2010;40:490–6.
17. Waki H, Tontonoz P. STAMPing out inflammation. Cell 2007;129:451–2.
18. Plenge RM, Cotsapas C, Davies L, Price AL, de Bakker PI, Maller J, et al. Two independent alleles at 6q23 associated with risk of rheumatoid arthritis. Nat Genet 2007;39:1477–82.
19. Thomson W, Barton A, Ke X, Eyre S, Hinks A, Bowes J, et al. Rheumatoid arthritis association at 6q23. Nat Genet 2007;39:1431–3.
20. Matmati M, Jacques P, Maelfait J, Verheugen E, Kool M, Sze M, et al. A20 (TNFAIP3) deficiency in myeloid cells triggers erosive polyarthritis resembling rheumatoid arthritis. Nat Genet 2011;43:908–12.
21. Lally F, Smith E, Filer A, Stone MA, Shaw JS, Nash GB, et al. A novel mechanism of neutrophil recruitment in a coculture model of the rheumatoid synovium. Arthritis Rheum 2005;52:3460–9.
22. Atsumi T, Ishihara K, Kamimura D, Ikushima H, Ohtani T, Hirota S, et al. A point mutation of Tyr-759 in interleukin 6 family cytokine receptor subunit gp130 causes autoimmune arthritis. J Exp Med 2002;196:979–90.
23. Murakami M, Okuyama Y, Ogura H, Asano S, Arima Y, Tsuruoka M, et al. Local microbleeding facilitates IL-6- and IL-17-dependent arthritis in the absence of tissue antigen recognition by activated T cells. J Exp Med 2011;208:103–14.
24. Tanaka Y, Matsumoto I, Iwanami K, Inoue A, Minami R, Umeda N, et al. Six-transmembrane epithelial antigen of prostate 4 (STEAP4) is a tumor necrosis factor α-induced protein that regulates IL-6, IL-8, and cell proliferation in synovium from patients with rheumatoid arthritis. Mod Rheumatol 2012;22:128–36.

ARD Online First, published on September 18, 2012 as 10.1136/annrheumdis-2012-201796

EXTENDED REPORT

Golimumab monotherapy in Japanese patients with active rheumatoid arthritis despite prior treatment with disease-modifying antirheumatic drugs: results of the phase 2/3, multicentre, randomised, double-blind, placebo-controlled GO-MONO study through 24 weeks

Tsutomu Takeuchi,[1] Masayoshi Harigai,[2] Yoshiya Tanaka,[3] Hisashi Yamanaka,[4] Naoki Ishiguro,[5] Kazuhiko Yamamoto,[6] Nobuyuki Miyasaka,[7] Takao Koike,[8] Minoru Kanazawa,[9] Takuya Oba,[10] Toru Yoshinari,[11] Daniel Baker,[12] the GO-MONO study group

▶ Additional data are published online only. To view these files please visit the journal online (http://dx.doi.org/10.1136/annrheumdis-2012-201796)

For numbered affiliations see end of article.

Correspondence to
Professor Tsutomu Takeuchi, Division of Rheumatology, Keio University, 35 Shinanomachi, Shinjuku-ku, Tokyo 160-8582, Japan;tsutake@z5.keio.jp

Accepted 21 August 2012

ABSTRACT

Objective To evaluate the efficacy and safety of golimumab 50 and 100 mg monotherapy in Japanese patients with active rheumatoid arthritis (RA) despite treatment with disease-modifying antirheumatic drugs (DMARDs).

Methods A total of 316 patients were randomised to receive subcutaneous injections every 4 weeks of placebo (group 1), golimumab 50 mg (group 2) or golimumab 100 mg (group 3); group 1 crossed over to golimumab 50 mg at week 16. The primary end point was the proportion of patients achieving ≥20% improvement in the American College of Rheumatology criteria (ACR20) at week 14. ACR50 and ACR70 response rates were also measured. Adverse events (AEs) were monitored throughout the study.

Results Demographics were similar across groups; the mean age was 52 years and 81.8% of patients (252/308) were female. Week 14 ACR20 response rates were significantly greater in groups 2 (51/101 (50.5%)) and 3 (60/102 (58.8%)) than in group 1 (20/105 (19.0%); $p<0.0001$ for both), as were ACR50 and ACR70 response rates. After placebo crossover at week 16, week 24 ACR response rates were similar in groups 1 and 2. Through week 16, 63.8% of patients in group 1, 62.4% in group 2 and 60.8% in group 3 had AEs and 1.9%, 1.0% and 2.0% had serious AEs. After week 16, one malignancy was reported (breast cancer, group 3). Infections were the most common AEs. No deaths or cases of tuberculosis were reported through week 24.

Conclusions Golimumab monotherapy (50 and 100 mg) was effective in reducing the signs and symptoms of RA in Japanese patients with active disease despite DMARD treatment.

INTRODUCTION

Rheumatoid arthritis (RA) is a chronic inflammatory disease characterised by dysregulation of several cytokines, including tumour necrosis factor (TNF).[1 2] The bone and cartilage damage in the joints can significantly affect physical function[3] and the chronic inflammation of RA is associated with significant morbidity and mortality.[4] In observational studies, the anti-TNF agents infliximab[5] and etanercept[6] reduced disease activity in Japanese patients with RA.

Golimumab is a monoclonal antibody that binds with high affinity and specificity to TNF[7] In large, phase 3, randomised, placebo-controlled trials, golimumab demonstrated efficacy in methotrexate (MTX)-naïve[8] and MTX-experienced patients with RA.[9] In these studies, many patients were treated with concomitant MTX. Some patients cannot tolerate MTX treatment[10]; therefore, it is clinically relevant to evaluate the safety and efficacy of golimumab monotherapy in Japanese patients with active RA who were previously treated with disease-modifying antirheumatic drugs (DMARDs).

PATIENTS AND METHODS

Patients

Patients (20–75 years) had to have a diagnosis of RA according to the American College of Rheumatology (ACR) criteria[11] for ≥3 months and active disease, despite previous DMARD treatment, defined as six or more swollen joints and six or more tender joints and two or more of the following: C-reactive protein (CRP) ≥2.0 mg/dl or erythrocyte sedimentation rate ≥28 mm/h using the Westergren method, morning stiffness ≥30 min, investigator-documented evidence of bone erosion on radiographs, or positive for anti-cyclic citrullinated peptide antibodies or rheumatoid factor. Patients were screened for latent and active tuberculosis (see also online supplementary text). All DMARDs were discontinued ≥4 weeks before the first study agent administration. Concomitant oral corticosteroids (stable dose ≤10 mg of prednisolone/day or equivalent) were permitted.

Study design

This was a phase 2/3 multicentre, randomised, double-blind, placebo-controlled trial carried out at 102 sites in Japan. Patients were randomly assigned (1:1:1) to receive subcutaneous injections every 4 weeks of placebo (group 1), golimumab 50 mg (group 2) or golimumab 100 mg (group 3). Concomitant DMARD treatment, including MTX, was prohibited in all treatment groups (a 4-week washout period was required). At week 16, all patients in group 1 crossed over to receive golimumab 50 mg in a double-blinded fashion.

The study was conducted according to the Declaration of Helsinki and in compliance with good clinical practice guidelines. The protocol was reviewed and approved by the institutional review board at each site. All patients provided written informed consent before any study-related procedures.

Study end points

Response to treatment was evaluated using the ACR criteria, the 28-joint count disease activity score (DAS28) using erythrocyte sedimentation rate and the ACR index of improvement in disease activity (ACR-N); physical function was evaluated with the Health Assessment Questionnaire-Disability Index (HAQ-DI). The primary end point was the proportion of patients achieving ≥20% improvement in ACR criteria (ACR20) at week 14. Due to ethical concerns about the potential for an inadequate response to placebo, week 14 was chosen for the primary efficacy assessment. Secondary end points included ACR50/70/90 response rates at weeks 14 and 24, changes from baseline at weeks 14 and 24 in DAS28 and HAQ-DI scores, ACR-N scores at weeks 14 and 24 and changes from baseline to week 24 in van der Heijde/Sharp (vdH–S) scores. Also the proportions of patients achieving a good or moderate DAS28 score[12 13] or DAS28 remission (score<2.6) were determined at weeks 14 and 24.

Radiographs of the hands and feet were obtained at baseline and week 24 or at the time of study discontinuation, if applicable, and scored by two independent readers (see online supplementary text). Radiographic progression was evaluated as changes from baseline to week 24 in the vdH–S score.[14] Erosion, joint space narrowing and total vdH–S scores are reported. All radiographs were scored by BioClinica Corporation (Newtown, Pennsylvania, USA) and readers were blinded to patient identity, treatment group and time point.

Patients were monitored for adverse events (AEs), including injection-site reactions and abnormal routine laboratory values.

Pharmacokinetic analyses and immunogenicity

Blood samples for the measurement of serum golimumab concentrations were obtained at weeks 0, 4, 8, 12, 14, 16, 20 and 24, with one additional sample between weeks 4 and 12. Blood samples for evaluation of antibodies to golimumab were obtained at weeks 0, 12 and 24. Antibodies to golimumab were detected using a previously described validated antigen bridging enzyme immunoassay.[15] Blood samples were drawn before administration of the study agent.

A post hoc analysis evaluated week 24 ACR20, ACR50 and ACR70 response rates for patients stratified according to the following serum golimumab concentration quartiles: <0.24 μg/ml, ≥0.24–<0.63 μg/ml, ≥0.63–<1.29 μg/ml and ≥1.29 μg/ml.

Statistical analyses

All patients who received at least one study agent injection and had efficacy data available were included in the efficacy analysis. All patients who received at least one study agent injection were included in the safety analysis. Patients who received one or more golimumab injection and had pharmacokinetic data available were included in the pharmacokinetic analysis. Descriptive statistics are reported. Differences between the treatment groups in ACR and DAS28 response rates were assessed using a χ^2 test. Type I error at the 0.05 level of significance was preserved with a hierarchical approach to control for multiplicity, in which a comparison between groups 3 and 1 was performed first and a comparison between groups 2 and 1 was performed only if the difference between groups 3 and 1 was significant. For changes in continuous variables, treatment group differences were assessed using analysis of covariance (ANCOVA) for HAQ-DI, DAS28 and vdH–S scores or analysis of variance (ANOVA) for ACR-N scores. Least-squares means and 95% CIs are reported. ACR response rates, ACR-N and HAQ-DI were calculated using the last observation carried forward method for the week 14 and week 24 time points. In the analysis of DAS28 response at weeks 14 and 24, observed data were used with no imputation for missing data, with the exception of the DAS28 remission analysis, in which patients with missing data were counted as non-responders. Observed data were used in the pharmacokinetic analysis.

Changes from baseline in vdH–S scores were compared between each golimumab group and placebo using two methods. ANCOVA was the prespecified method in the protocol and was chosen for consistency with the analyses of other continuous variables. A post hoc ANOVA based on van der Waerden normal scores was undertaken to account for the non-normal data distribution due to one patient in group 3 with an atypically large change in vdH–S score. Additionally, a cumulative probability plot of the changes in vdH–S scores from baseline to week 24 for each treatment group was constructed.

Assuming that 5% of patients would be excluded from the efficacy analysis owing to study discontinuation, the target total sample size of 300 patients provided >90% power to detect a difference between groups 2 and 3 and group 1 in ACR20 response rates at week 14 (α=0.05).

RESULTS

Patient disposition and baseline characteristics

A total of 316 patients were randomised; eight withdrew consent before administration of any study agents (figure 1). Therefore, 308 patients received one or more study agent administration (group 1, n=105; group 2, n=101; group 3, n=102). Patient demographics and baseline disease characteristics were well balanced across all groups (table 1). Among all patients, 82% were female, the mean age was 52 years, the mean disease duration was 8.9 years and the mean CRP level was 2.5 mg/dl. Most (73.7%) patients received prior MTX treatment.

Efficacy results

Clinical response and physical function

At week 14, significantly greater proportions of patients in groups 2 (50.5%) and 3 (58.8%) achieved an ACR20 response in comparison with group 1 (19.0%; p<0.0001 for both) (table 2). Likewise, significantly higher ACR50 and ACR70 response rates were seen in groups 2 and 3 than in group 1. While no patient in group 1 had an ACR90 response at week 14, three patients in group 2 and two in group 3 achieved an ACR90 response; however, statistical significance from placebo was not attained.

At week 24, after placebo crossover to golimumab 50 mg at week 16, patients in group 1 generally had ACR response rates

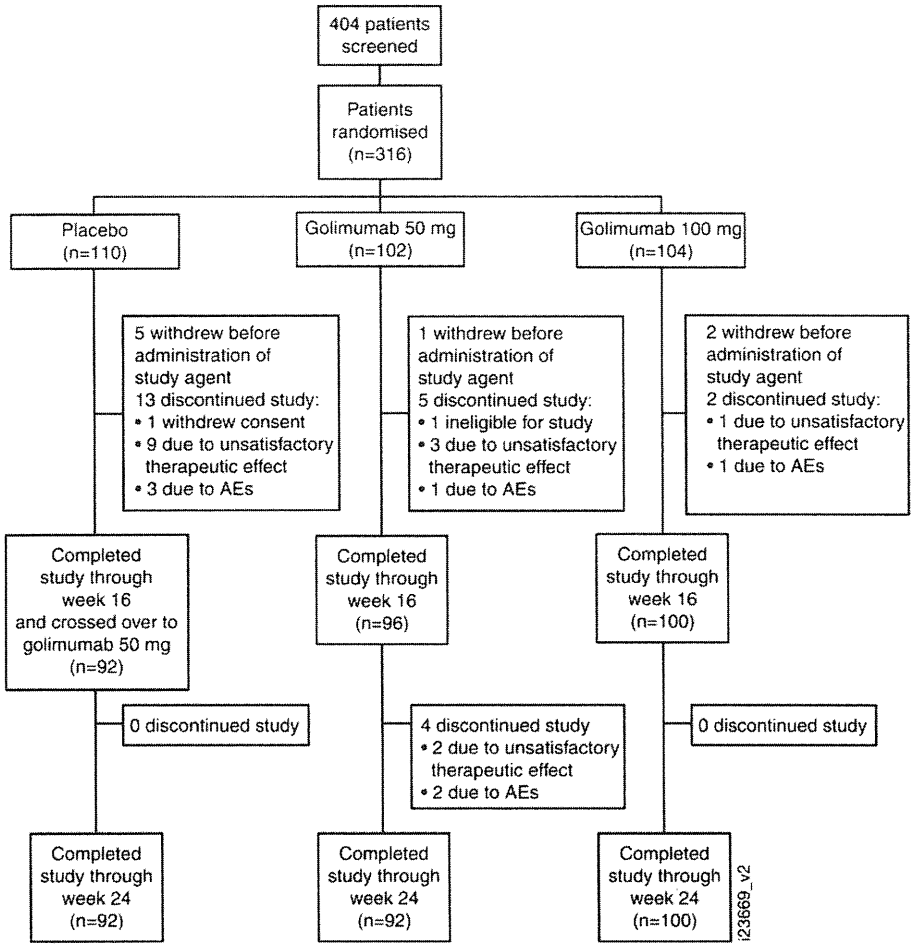

Figure 1 Patient disposition through week 24. AE, adverse event.

similar to those for patients who were initially assigned to group 2 from baseline (table 2). In group 3, week 14 ACR response rates were maintained at week 24.

Mean ACR-N scores at week 14 were significantly greater in groups 2 (30.5) and 3 (33.0) than in group 1 (9.1; $p<0.0001$ for both) (table 2). Mean improvements from baseline to week 14 in DAS28 scores were also significantly greater in groups 2 and 3 than in group 1 and significantly greater proportions of patients in groups 2 and 3 achieved a moderate or good DAS28 response or DAS28 remission. Improvements from baseline in physical function (HAQ-DI) were also significantly greater in groups 2 and 3 than in group 1.

Patients in group 1 had ACR-N scores at week 24 and mean improvements in DAS28 and HAQ-DI scores from baseline to week 24 that were similar to those seen in patients who were initially randomised to group 2. In group 3, week 14 ACR-N, DAS28 and HAQ-DI responses were maintained at week 24.

Radiographic progression

Two patients did not have complete radiographic data available (missing baseline data for one patient in group 3 and missing week 24 data for one patient in group 2) and changes from baseline in vdH–S score for these patients were substituted with the median change for all patients. Agreement between the two primary readers was good, with intraclass correlation coefficients of 0.98 at baseline and week 24 and 0.80 for the change at week 24. The proportion of patients with a change in total vdH–S score greater than the smallest detectable change was 22.1% (group 1, n=27; group 2, n=21; group 3, n=20).

At week 24, increases in erosion, joint space narrowing and total vdH–S scores were seen in all three groups (table 2), with smaller changes in erosion and total scores in groups 2 and 3, indicating less radiographic progression than in group 1, as shown in the probability plot (figure 2). In the a priori analysis (ANCOVA), no significant differences were seen in mean changes between groups 2 and 3 and group 1 at week 24. In the post hoc ANOVA using normalised scores, no significant differences were seen between groups 2 and 1. Although increases from baseline were observed in both groups 3 and 1, the mean changes in erosion and total vdH–S scores in group 3 were statistically significantly smaller than those in group 1 (1.1 vs 1.3, $p=0.0316$ and 2.1 vs 2.6, $p=0.0043$, respectively). Also, the median changes in total vdH–S scores followed a trend, showing less radiographic progression in groups 2 and 3 than in group 1 (0.5 and 0.0, respectively, vs 1.0).

Golimumab pharmacokinetics and antibodies to golimumab

Through week 16, serum golimumab levels increased in a dose-proportional manner; steady state was reached at week 12. Median serum golimumab concentrations for groups 2 and 3, respectively, were 0.52 μg/ml and 1.17 μg/ml at week 12 and

Table 1 Baseline patient demographics and disease characteristics

Characteristics	Group 1: Placebo	Group 2: Golimumab 50 mg	Group 3: Golimumab 100 mg	Total
Patients, n	105	101	102	308
Female, n (%)	86 (81.9)	81 (80.2)	85 (83.3)	252 (81.8)
Age, years	52.4 (11.1)	52.9 (11.3)	51.6 (11.9)	52.3 (11.4)
Body weight, kg	54.4 (10.4)	56.2 (12.4)	53.9 (9.8)	54.8 (10.9)
Duration of RA, years	9.2 (8.6)	8.1 (8.4)	9.4 (8.5)	8.9 (8.5)
Swollen joint count (0–66)	13.1 (6.9)	12.6 (5.8)	12.9 (6.7)	12.9 (6.5)
Tender joint count (0–68)	14.9 (8.5)	15.5 (9.0)	16.6 (10.2)	15.7 (9.3)
Patient's assessment of pain (VAS; 0–100 mm)	55.2 (24.5)	55.6 (22.3)	57.5 (23.1)	56.1 (23.3)
Patient's global assessment (VAS; 0–100 mm)	54.3 (25.4)	54.3 (23.7)	53.9 (24.5)	54.2 (24.5)
Physician's global assessment (VAS; 0–100 mm)	58.8 (17.8)	58.4 (18.1)	59.6 (18.3)	58.9 (18.0)
CRP, mg/dl	2.5 (2.5)	2.2 (2.5)	2.6 (2.8)	2.5 (2.6)
DAS28-ESR	5.9 (1.0)	5.8 (1.1)	6.0 (1.0)	5.9 (1.0)
HAQ-DI (0-3)	1.0 (0.6)	1.1 (0.6)	1.0 (0.6)	1.0 (0.6)

Data are presented as mean (SD) unless otherwise noted.
Results include data for all randomised patients who received at least one administration of the study agent and had available efficacy data.
CRP, C-reactive protein; DAS28-ESR, 28-joint Disease Activity Score using erythrocyte sedimentation rate; HAQ-DI, Health Assessment Questionnaire-Disability Index; RA, rheumatoid arthritis; VAS, visual analogue scale.

0.46 μg/ml and 1.04 μg/ml at week 16. Median serum concentrations at week 24 were 0.35 μg/ml in group 1, 0.43 μg/ml in group 2 and 0.99 μg/ml in group 3. Week 24 ACR20, ACR50 and ACR70 response rates were evaluated according to serum golimumab concentration, with patients stratified by the following quartiles: <0.24 μg/ml (n=45), ≥0.24–<0.63 μg/ml (n=50), ≥0.63–<1.29 μg/ml (n=49) and ≥1.29 μg/ml (n=48). Overall, response rates were lowest in patients with serum golimumab concentrations <0.24 μg/ml and increased with increasing serum golimumab concentration (figure 3).

At week 12, two patients (2.0%) each in groups 2 and 3 tested positive for antibodies to golimumab. At week 24, three patients each in group 1 (3.3%) and group 2 (3.2%) and four patients (4.0%) in group 3 tested positive for antibodies to golimumab. No antibody-positive patient demonstrated an ACR response.

Adverse events

Through week 16 (placebo-controlled period), AEs occurred in 63.8% of patients in group 1, 62.4% in group 2 and 60.8% in group 3 (table 3). Most AEs were mild. The most common AEs were infections (group 1 (23.8%); group 2 (26.7%); group 3 (28.4%)). The most common infections among all golimumab-treated patients were nasopharyngitis (16.3%), pharyngitis (3.4%) and gastroenteritis (2.0%). Three patients (2.9%) in group 1 (herpes zoster, atypical mycobacterial infection and abnormal liver function test), two patients (2.0%) in group 2 (liver disorder and cataract) and one patient (1.0%) in group 3 (transient cerebral ischaemic attack) discontinued the study agent owing to AEs. Serious AEs (SAEs) through week 16 were herpes zoster and organising pneumonia (n=1 each) in group 1, hydrocele (n=1) in group 2 and cellulitis and transient ischaemic attack (n=1 each) in group 3. When assessed by length of follow-up, the incidences (95% CI) of serious infection at week 24 were 3.30 (0.08 to 18.38), 1.69 (0.04 to 9.40) and 2.16 (0.05 to 12.01) for groups 1, 2 and 3, respectively.

After the placebo crossover at week 16, AEs occurred in 31 (33.7%) patients in group 1, 34 (35.4%) in group 2 and 33 (33.0%) in group 3 through week 24 (table 3). Infections were the most common AEs during this time period, consistent with results seen during the placebo-controlled period. AEs leading to discontinuation of the study agent after week 16 were ovarian neoplasm (non-malignant; n=1) and RA (n=1) in group 2 and breast cancer (n=1) in group 3. After week 16, SAEs occurred in three patients in group 2 (non-malignant ovarian neoplasm and dental pulpitis, each in one patient; paroxysmal tachycardia and RA in one patient) and in two patients in group 3 (breast cancer, between weeks 20 and 24 and organising pneumonia, one patient each); no SAEs were reported in group 1 during this period.

The incidence of injection-site reactions through week 16 was similar among all groups (group 1, 7/105 (6.7%); group 2, 8/101 (7.9%); group 3, 8/102 (7.8%)). From week 16 through week 24, the rates of injection-site reactions were 3.3% (3/92) in group 1, 6.3% (6/96) in group 2 and 5.0% (5/100) in group 3. All injection-site reactions were mild.

There were no reports of anaphylactic reactions, serum sickness-like reactions, or deaths through week 24. No cases of tuberculosis were reported through week 24; however, one case of atypical mycobacterial infection occurred in group 1 before week 16.

DISCUSSION

In this phase 2/3 study of golimumab 50 mg and 100 mg in Japanese patients with active RA despite DMARD treatment, those treated with golimumab monotherapy had significant improvements from baseline to week 14 in clinical measures of efficacy, including ACR20, ACR50 and ACR70 response rates and DAS28 and ACR-N scores, in comparison with those who received placebo. Physical function was also significantly improved from baseline in the golimumab groups compared with placebo. These significant improvements were seen despite the overall study population displaying relatively mild disease at study outset (mean swollen/tender joint counts of 13/16). However, clinical response to golimumab monotherapy was relatively modest in comparison with golimumab+MTX treatment in another Japanese population.[16]

Patients with active RA despite previous MTX treatment were evaluated previously in the large phase 3 GO-FORWARD trial.[9] While concomitant MTX was included in GO-FORWARD golimumab 100 mg monotherapy was also evaluated. ACR responses were also evaluated at week 14 in both trials and while significantly greater ACR response rates were achieved in group 3 in this study in comparison with placebo,

Table 2 Clinical efficacy and radiographic results† through week 24

	Placebo-controlled period			Placebo crossover period		
	Week 14			Week 24		
	Group 1: Placebo (n=105)	Group 2: Golimumab 50 mg (n=101)	Group 3: Golimumab 100 mg (n=102)	Group 1: Placebo→Golimumab 50 mg (n=105)	Group 2: Golimumab 50 mg (n=101‡)	Group 3: Golimumab 100 mg (n=102)
Clinical efficacy results						
ACR20 response	20 (19.0)	51 (50.5) p<0.0001	60 (58.8) p<0.0001	18 (17.1)	47 (46.5) p<0.0001	71 (69.6) p<0.0001
ACR50 response	6 (5.7)	29 (28.7) p<0.0001	33 (32.4) p<0.0001	8 (7.6)	28 (27.7) p=0.0001	43 (42.2) p<0.0001
ACR70 response	1 (1.0)	13 (12.9) p=0.0007	12 (11.8) p=0.0013	2 (1.9)	17 (16.8) p=0.0002	22 (21.6) p<0.0001
ACR90 response	0 (0.0)	3 (3.0) p=0.0752	2 (2.0) p=0.1493	0	5 (5.0) p=0.021	3 (2.9) p=0.0767
ACR-N	9.1 (4.3 to 14.0)	30.5 (25.6, 35.5) p<0.0001	33.0 (28.1, 38.0) p<0.0001	9.3 (3.9, 14.7)	30.9 (25.4, 36.4) p<0.0001	40.0 (34.6, 45.5) p<0.0001
DAS28-ESR						
Change from baseline	n=94 −0.3 (−0.6 to −0.1)	n=97 −1.5 (−1.8, −1.3) p<0.0001	n=100 −1.9 (−2.1 to −1.7) p<0.0001	n=91 −1.5 (−1.8, −1.2)	n=93 −1.6 (−1.9 to −1.4)	n=100 −1.9 (−2.1, −1.6)
Moderate response	n=93 27 (29.0)	n=97 69 (71.1) p<0.0001	n=100 74 (74.0) p<0.0001	n=91 56 (61.5)	n=93 65 (69.9)	n=100 78 (78.0)
Good response	n=93 4 (4.3)	n=97 23 (23.7) p=0.0001	n=100 32 (32.0) p<0.0001	n=91 21 (23.1)	n=93 21 (22.6)	n=100 31 (31.0)
Remission	n=94 2 (2.1)	n=97 13 (13.4) p=0.0025	n=100 23 (23.0) p<0.0001	n=92 8 (8.7)	n=93 16 (17.2)	n=100 19 (19.0)
HAQ-DI						
Change from baseline	−0.03 (−0.12 to 0.06)	0.24 (0.15 to 0.34) p<0.0001	0.33 (0.24 to 0.42) p<0.0001	−0.03 (−0.13 to 0.07)	0.23 (0.13 to 0.33) p=0.0003	0.33 (0.23 to 0.43) p<0.0001
Radiographic results						
vdH–S score, baseline						
Total	–	–	–	56.1 (62.2)	43.8 (50.6)	56.9 (57.0)
Joint space narrowing	–	–	–	25.9 (30.2)	19.9 (24.0)	25.3 (26.2)
Erosion	–	–	–	30.2 (33.8)	23.9 (28.3)	31.7 (33.0)
vdH–S score, change from baseline to week 24						
Total				n=105 2.6 (4.7) 1.0 (−2.5 to 29.8)	n=100 1.9 (4.1) 0.5 (−1.8 to 23.0) p=0.5091* p=0.1802**	n=102 2.1 (10.4) 0.0 (−2.5 to 102.5) p=0.6573* p=0.0043**
Joint space narrowing				n=92 0.9 (1.9) 0.0 (−1.0 to 9.5)	n=93 1.0 (2.8) 0.0 (−1.5 to 17.5) p=0.7530* p=0.3373**	n=99 1.0 (5.1) 0.0 (−2.0 to 48.5) p=0.9353* p=0.0832**

Continued

Table 2 Continued

	Placebo-controlled period			Placebo crossover period		
	Week 14			Week 24		
	Group 1: Placebo (n=105)	Group 2: Golimumab 50 mg (n=101)	Group 3: Golimumab 100 mg (n=102)	Group 1: Placebo→Golimumab 50 mg (n=105)	Group 2: Golimumab 50 mg (n=101‡)	Group 3: Golimumab 100 mg (n=102)
Erosion						
				n=92	n=93	n=99
				1.3 (2.5)	1.0 (2.1)	1.1 (5.7)
				0.5 (−2.5 to 14.5)	0.5 (−1.5 to 11.5)	0.0 (−2.5 to 54.0)
					p=0.6272*	p=0.7614*
					p=0.5895**	p=0.0316**

*p Values based on analysis of covariance on least-squares mean and two-sided 95% CIs with treatment and baseline value as covariates.
**p Values based on analysis of variance on van der Waerden normal scores.
†Clinical efficacy data are presented as n (%) or least-squares mean (95% CI). Radiographic data are presented as mean (SD) and median (range).
‡Data from one patient who discontinued the study before week 24 were included in these analyses because the timing of the study termination visit fell within the prespecified time period for week 24 data collection.
ACR20/50/70/90, 20%/50%/70%/90% improvement in the American College of Rheumatology criteria; ACR-N, American College of Rheumatology index of improvement; DAS28-ESR, 28-joint Disease Activity Score using erythrocyte sedimentation rate; HAQ-DI, Health Assessment Questionnaire-Disability Index; vdH-S, van der Heijde/Sharp.

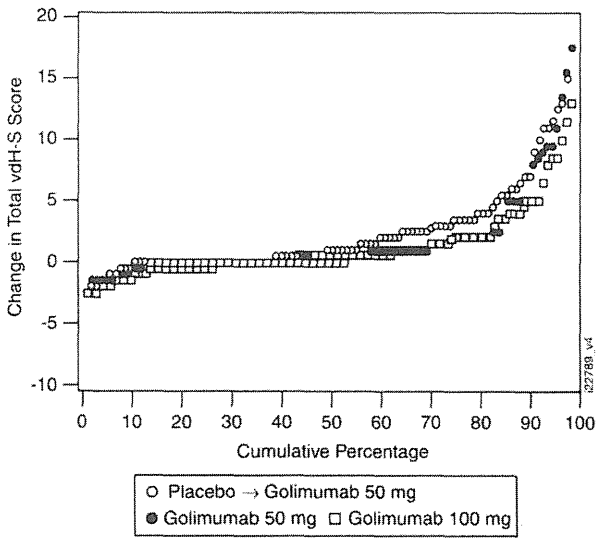

Figure 2 Cumulative probability plot of changes in van der Heijde-Sharp (vdH–S) scores from baseline to week 24 Data from one patient in the golimumab 100 mg group who had an atypically large change in vdH–S score were excluded.

the primary end point was not achieved in the golimumab 100 mg monotherapy group in the GO-FORWARD trial. Possible explanations for the non-statistically significant response in the GO-FORWARD 100 mg monotherapy group were previously described (eg, the relatively low disease activity in the trial population and the high response rate in the MTX monotherapy group).[9] However, factors such as patient body weight, which is known to affect the pharmacokinetic properties of monoclonal antibodies,[17–19] may also account for the difference in response seen in the two trials. While a previous study found no apparent differences in the pharmacokinetic parameters of golimumab in healthy body-weight-matched Caucasian and Japanese male subjects,[20] it is possible that the body weights of patients in 100 mg monotherapy groups in

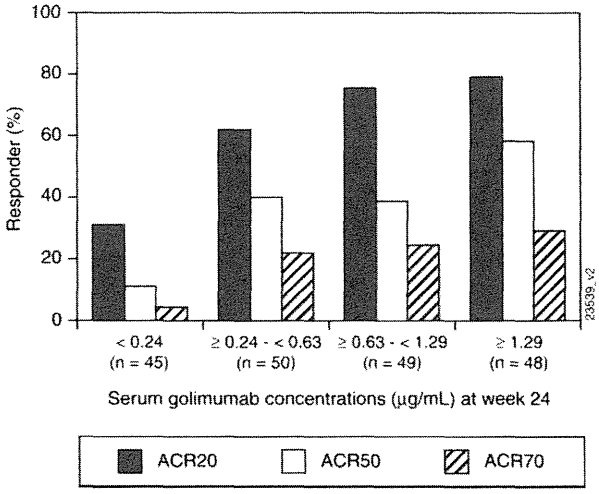

Figure 3 The proportions of patients achieving an ACR20, ACR50 and ACR70 responses stratified by serum golimumab concentration quartiles (µg/ml) at week 24. ACR20/50/70, 20%/50%/70% improvement in the ACR criteria.

Table 3 Week 16 and week 24 safety results

	Placebo-controlled period			Placebo crossover period			Cumulative	
	Weeks 0–16			Weeks 16–24			Weeks 0–24	
	Group 1: Placebo	Group 2: Golimumab 50 mg	Group 3: Golimumab 100 mg	Group 1: Placebo→Golimumab 50 mg	Group 2: Golimumab 50 mg	Group 3: Golimumab 100 mg	Group 2: Golimumab 50 mg	Group 3: Golimumab 100 mg
Patients, n	105	101	102	92	96	100	101	102
Patients with AEs	67 (63.8)	63 (62.4)	62 (60.8)	31 (33.7)	34 (35.4)	33 (33.0)	72 (71.3)	72 (70.6)
Patients with SAEs	2 (1.9)	1 (1.0)	2 (2.0)	0 (0)	3 (3.1)	2 (2.0)	4 (4.0)	4 (3.9)
Patients with AEs leading to discontinuation of study agent	3 (2.9)	2 (2.0)	1 (1.0)	0 (0)	2 (2.1)	1 (1.0)	4 (4.0)	2 (2.0)
Patients with infections	25 (23.8)	27 (26.7)	29 (28.4)	5 (5.4)	11 (11.5)	7 (7.0)	33 (32.7)	34 (33.3)
Patients with serious infections	1 (1.0)	0 (0)	1 (1.0)	0 (0)	1 (1.0)	0 (0)	1 (1.0)	1 (1.0)
Patients with abnormal LFTs	3 (2.9)	0 (0)	4 (3.9)	0 (0)	0 (0)	0 (0)	0 (0)	4 (3.9)
Patients with injection-site reactions	7 (6.7)	8 (7.9)	8 (7.8)	3 (3.3)	6 (6.3)	5 (5.0)	12 (11.9)	10 (9.8)
Patients with neoplasms (benign, malignant and unspecified)	0 (0)	0 (0)	0 (0)	0 (0)	2 (2.1)	1 (1.0)	2 (2.0)	1 (1.0)
Breast cancer	0 (0)	0 (0)	0 (0)	0 (0)	0 (0)	1 (1.0)	0 (0)	1 (1.0)
Skin papilloma	0 (0)	0 (0)	0 (0)	0 (0)	1 (1.0)	0 (0)	1 (1.0)	0 (0)
Ovarian neoplasm	0 (0)	0 (0)	0 (0)	0 (0)	1 (1.0)	0 (0)	1 (1.0)	0 (0)

Data are presented as n (%) unless otherwise noted.
AEs, adverse events; LFT, liver function test; SAEs, serious adverse events.

this trial and in GO-FORWARD might have varied considerably[21] given that Japanese patients are generally more slight, and the resulting dose per unit mass would be higher than in other populations. Indeed, treatment effects on radiographic progression appear to be related to serum golimumab concentrations, as patients receiving golimumab 50 mg+MTX in the GO-FORTH trial in Japanese patients with RA (week 16 median serum golimumab concentration=0.73 μg/ml) demonstrated significantly less radiographic progression than placebo-treated patients,[16] while such a difference was not seen in this study, in which patients receiving golimumab 50 mg had a week 16 median serum golimumab concentration of 0.46 μg/ml.

Radiographic progression was evaluated at week 24, at which point patients randomised to group 1 had been receiving golimumab 50 mg since week 16. The a priori ANCOVA did not show significant differences in radiographic progression between either groups 2 or 3 and group 1; however, in a post hoc analysis using normalised data, significantly smaller changes from baseline in erosion and total vdH–S scores were seen in group 3 than in group 1. This significant difference was confirmed by an additional ANCOVA that excluded a single group 3 patient with an atypically large change in vdH–S score ($p=0.01$; data not shown). Biological monotherapy with the anti-interleukin 6 agent tocilizumab has also demonstrated radiographic benefit in patients with RA with inadequate response to DMARD treatment.[22] In this study, the mean baseline CRP level, which is a good predictor of radiographic progression,[23] was moderately raised and 22.1% of patients had a change in total vdH–S that exceeded the smallest detectable change. In contrast, only 4.3% of patients in GO-FORWARD had such a change in total vdH–S score.[24] Thus, patients in our study probably had higher disease activity than patients in GO-FORWARD. This may account for the observation that radiographic progression in this study was greater than expected based on the clinical response seen at similar time points in earlier golimumab trials, including GO-FORWARD.[24] Our results suggest that golimumab 100 mg monotherapy may prevent further joint damage in Japanese patients with active radiographic progression, which is consistent with the golimumab package insert approved by the Japanese Pharmaceuticals and Medical Devices Agency.[25]

Golimumab was generally well tolerated. Infections were the most common AEs. Serious infections were reported in two patients through week 16 and one patient between weeks 16 and 24; the week 24 incidences per 100 patient-years of follow-up indicated no increase in serious infection versus placebo. Most AEs were mild and few patients discontinued due to AEs. Rates of SAEs, serious infections and malignancies were low. No deaths and one malignancy (breast cancer) occurred through week 24. Of note, this study was not powered to detect rare events and these findings are limited also by the short-term nature of the analysis.

This was the first golimumab monotherapy study to demonstrate that Japanese patients with active RA despite prior DMARD treatment had significantly improved signs and symptoms of RA after 14 weeks of treatment with 50 or 100 mg golimumab in comparison with placebo. Group 3 had significantly less radiographic progression than group 1 when analysed post hoc using normalised scores, and median changes in total vdH–S scores suggested a dose-dependent trend. Additional long-term analyses are needed to further explore the effect of golimumab monotherapy on joint destruction and fully assess its safety profile in Japanese patients with RA.

Author affiliations
[1]Division of Rheumatology, Keio University, Shinjuku-ku, Tokyo, Japan
[2]Department of Pharmacovigilance, Graduate School of Medical and Dental Sciences, Tokyo Medical and Dental University, Bunkyo-ku, Tokyo, Japan
[3]First Department of Internal Medicine, University of Occupational and Environmental Health, Kitakyushu, Fukuoka, Japan
[4]Institute of Rheumatology, Tokyo Women's Medical University, Shinjuku-ku, Tokyo, Japan
[5]Department of Orthopedic Surgery, Nagoya University, Nagoya, Aichi, Japan
[6]Department of Allergy and Rheumatology, Graduate School of Medicine, The University of Tokyo, Bunkyo-ku, Tokyo, Japan
[7]Department of Medicine and Rheumatology, Graduate School of Medical and Dental Sciences, Tokyo Medical and Dental University, Bunkyo-ku, Tokyo, Japan
[8]Sapporo Medical Center NTT EC, Sapporo, Japan
[9]Respiratory Center, Saitama medical University, Moroyama-machi, Iruma-gun, Saitama, Japan
[10]Janssen Pharmaceutical K.K., Chiyoda-ku Tokyo, Japan
[11]Mitsubishi Tanabe Pharma Corporation, Chuo-ku Tokyo, Japan
[12]Janssen Research & Development, LLC, Spring House, Pennsylvania, USA

Acknowledgements We thank the patients, investigators and study personnel who made this trial possible. We also thank Rebecca Clemente, PhD, Michelle Perate,